Geohazard Assessment of Five Deepwater Pipeline Scenarios on the Scotian Slope

D. Calvin Campbell and Adam W.A. MacDonald

Geological Survey of Canada Open File # 5079

2006

Natural Resources Canada | Ressources naturelles Canada

Canada

GEOLOGICAL SURVEY OF CANADA

OPEN FILE # 5079

Geohazard Assessment of Five Deepwater Pipeline Scenarios on the Scotian Slope

D. Calvin Campbell and Adam W.A. MacDonald

2006

Available from
Geological Survey of Canada
Bedford Institute of Oceanography
1 Challenger Drive
Dartmouth, Nova Scotia B2Y 4A2

Campbell D.C. and MacDonald, A.W.A.
2006: Geohazard Assessment of Five Deepwater Pipeline Scenarios on the Scotian Slope, Geological Survey of Canada, Open File # 5079, 48 p.

Open files are products that have not gone through the GSC formal publication process.

Table of Contents

Introduction

As worldwide oil and gas exploitation moves towards deepwater, there has been an increased demand for the development of new technologies for transporting the resource to market. One of the more common modes chosen is subsea tiebacks from deepwater and ultradeepwater fields to existing infrastructure on the continental shelf by way of pipelines. In some cases, anchored production facilities are positioned offshore in the field area and pipelines transport processed hydrocarbons to shore, for example the Mardi Gras network in the Gulf of Mexico (Marshall and McDonald, 2004). In other cases the entire field infrastructure is subsea and is controlled from production facilities onshore, with pipelines transporting raw hydrocarbons and associated fluids, for example the Ormen Lange development in the Norwegian Sea (Henriksson, 2004).

Selecting a pipeline route is a complex process governed by primary and secondary factors (Tootill et al. 2004). Primary factors include the start and end positions of the pipeline; i.e. the position of the gas/oil field and the destination of the pipeline are fixed, and the route selection is limited by the installation parameters of the pipeline. Secondary factors include bathymetry and seabed conditions, geohazards, bio-environmental issues, and existing infrastructure. The challenge is to create the shortest and, therefore, least expensive route allowable by the primary and secondary factors.

On the Scotian Slope, twelve exploratory wells have been drilled in deepwater, with seven wells drilled in the latest round of exploration activity, 2001- 2004. In 2002, a gas discovery was made at the Annapolis G-24 site, which is located east of Logan Canyon in 1678 m water depth (Figure 1). To date no pipelines have been installed on the Scotian Slope. Therefore it is an appropriate time to evaluate conceptual routes before specific route surveys are conducted. Concepts derived from this evaluation will be applicable to other areas of the Scotian Slope, and even other areas of the eastern Canadian margin.

The purpose of this study is to assess geological constraints to pipeline placement along five deepwater pipeline route scenarios on the Scotian Slope. The study provides detailed seabed topography analysis and surficial geology interpretation along the routes. It also presents a review of other geological factors which may affect design planning and feasibility, both for installation and operation, such as sediment mobility, sediment

stability, bottom currents, and seismicity. This study does not provide specific recommendations for pipeline placement within the study area.

Criteria for Geohazard Assessment

Detailed knowledge of seabed conditions and shallow geology are required for proper pipeline route selection and for siting associated tie-in structures (Tootill et al., 2004). In deepwater areas, the primary areas of concern are factors leading to pipeline buckling during installation and geohazards during operation (Carr and Preston, 1999). Typical geohazard factors to be considered for route selection include, but are not limited to: unstable seabed, subsidence, rugged topography, turbidity flows, seismic activity, evidence of sediment transport, pockmarks, boulder fields, and rock outcrops (DNV, 2004).

Methods

This study uses new data analysis and review of existing literature to provide a geohazard assessment for the five pipeline route scenarios. Multibeam bathymetry, high resolution seismic reflection profiles, and piston cores were analyzed to assess seabed conditions along each routes. A detailed review of the datasets used is given in Mosher et al. (2004).

Multibeam Sonar

In excess of 22,000 km^2 of multibeam sonar hydrographic data were acquired as part of the Scotian Slope geohazard program (Mosher et al. 2004). Multibeam data were collected using Simrad EM300 and EM1002 multibeam sonar systems. The EM300 system operates at 30 kHz, making it capable of surveying in water depths to 4500 m below the transducer. The resolution of the system varies with water depth and grazing angle, but as an example, at 1500 m water depth, the footprint of an individual beam is about 53 m wide while the beam spacing directly below the vessel is 22 m, giving

considerable overlap between beams. Therefore, the best resolution in an ideal setting is approximately 22 m in 1500 m of water, with increased resolution in shallower water and with decreased resolution in deeper water and towards the outer beams (increased grazing angle). The EM1002 operates at 95 kHz and the system is capable of working in water depths from 3 to 1000 m. Horizontal resolution is on the order of 5 m in 100 m water depth and vertical resolution on the order of 0.25 m, but again these estimates vary with water depth and ensonification angle.

Seismic Reflection Data

Seismic reflection data consisted of mainly Huntec DTS sparker profiles. The system consists of a tow fish towed up 100 m below the sea surface with data recorded on a short, single channel array. The centre frequency for the Huntec sparker is about 1500 Hz and spans from 500-2500 Hz. The maximum vertical resolution is, therefore, about 0.20 m (Mosher et al. 2004).

Piston Cores and Sediment Physical Properties

The piston coring system used in this study was a Long Corer Facility (LCF) (Driscoll et al., 1989) with a 1 tonne core head. This device obtains a 10 cm-diameter, up to 15 m long sediment core sample. Sediment bulk density and undrained shear strength were measured at the ends of each core section (≤1.5 m-interval) immediately upon recovery of the core. All cores were sealed and kept upright in refrigerated storage for shore-based analysis. Each core was passed through a multi-sensor track (MST) before splitting. The MST measures magnetic susceptibility, gamma ray attenuation (bulk density) and compressional-wave acoustic velocity. After splitting, the cores were photographed, visually described and measured for a suite of physical properties, including index properties (bulk density, dry density, water content, porosity), color reflectance, shear strength, and acoustic velocity. Atterberg limits testing and full grain size analysis were conducted on selected samples (Mosher et al, 2004).

Pipeline Route Scenario Selection

Five pipeline route scenarios were investigated in this study (Figure 2). All routes are from deepwater (1600-1700 m) to the outer continental shelf (150-200 m). Scenarios 1-3 traverse from the Annapolis field to the outer shelf. Route 1 is a straight line route from the Annapolis G-24 location to the outer shelf. Route 2 is a route which follows an intercanyon ridge to the outer shelf. Route 3 traverses laterally down a ridge and then follows a canyon floor to the outer shelf. Routes 4 and 5 traverse from an arbitrary location on the slope to the shelf and were chosen to compare similarities and differences between the general area of routes 1-3 with another area. Route 4 follows a particularly narrow canyon ridge from the arbitrary location. Route 5 follows a canyon floor to the outer shelf from the arbitrary location.

Detailed Seabed Morphology Analysis

The multibeam data were gridded at 20 m cell spacing in order to create a continuous digital terrain model (D.T.M.) for the study area (Figure 2). A gradient surface was created from the D.T.M. (Figure 2). Gradient values were derived for each cell by fitting a plane through the surrounding eight cells which resulted in both a slope angle for the cell and a direction of dip or azimuth (McCoy and Johnston, 2001). Traditionally the standard procedure has been to artificially shade the D.T.M. to enhance bathymetric features, however, for this study, gradient angle coloured from white (shallow slope) to black (steep slope) was draped over seafloor elevation. This method removed some of the positional biases associated with artificial shading and allowed for more accurate selection of pipeline route scenarios.

Routes were digitised in ArcGIS™ as polylines. For each route, a profile of seafloor elevation was derived from the multibeam and a profile of seabed gradient angle was derived from the gradient surface. The technique resulted in a point theme, with a point created for each cell of the D.T.M. that the route intersected. Since the final resting position of a pipeline on the seafloor may differ slightly from the planned route, it was decided that statistics on seabed variability within close proximity to each route scenario should be evaluated. To do this, a 200 m diameter buffer was created around each point

in the route and slope angle statistics were compiled for the cells within each buffered area. Each buffered area enveloped 78-80 cells. Seafloor gradient statistics were compiled for the buffered regions along the route into a database. The statistics included maximum, minimum, mean and median gradient, and standard deviation. Graphs were prepared for each route that show surficial geology, bathymetric profile, and seafloor gradient profile, median slope angle within a 200 m wide corridor, and standard deviation or variability within the corridor.

RESULTS

Surficial Geology

The surficial geology of the study area was mapped in detail based on available geophysical and groundtruth data (Figure 3). Except for the upper slope, most of the Scotian Slope is draped with a centimetre to metre thick layer of Holocene mud. In general on the Scotian Slope, upper slope till passes downslope into stratified sediments of Pleistocene age. In places the stratified sediments are incised by submarine canyons and channels. The upper limit of seabed failure and erosion commonly coincides with the downslope limit of till. The study area consists of seven surficial geological types described below:

Canyon head deposits

Canyon head deposits consist of predominantly overconsolidated mud, in places with lesser silt and sand, formed through the burial and diagenesis of proglacial and hemipelagic sediment and subsequent exposure through headward erosion of a canyon. Based on cores and sub-bottom profiles, the seabed within canyon heads is variable, consisting of silty mud to sandy gravel over more competent substrate (Figure 4, Figure 5). Piper and Campbell (2002) showed that canyon heads in the study area are eroded (Figure 6).

Canyon wall deposits

Canyon wall deposits consist of predominantly overconsolidated mud formed through the burial and diagenesis of proglacial and hemipelagic sediment and subsequent exposure through gully erosion, mass transport erosion and down-canyon erosive flows. Canyon wall morphology ranges from well developed ridge and gully topography to terraced or smooth relief. ROV observations show that canyon walls consist of subvertical. partially lithified mudstones and shales, as well as flatter areas which accumulate recent sediments (Piper and Campbell, 2002). In 2000, several attempts were made to piston core canyon walls with little success (Mosher, 2000-042 cruise report), resulting in damaged coring equipment. The cores that recovered sediment consist of a drape of Holocene mud over stiffer older sediment (Figure 7). Canyon walls are poorly imaged on sub-bottom profiles due to their steepness (Figure 8).

Ice-margin deposits

Ice-margin deposits consist of acoustically incoherent glacial diamict with interbedded mud and sand, deposited at the seaward limit of glaciers during glacial periods. It outcrops on the upper slope between 300 m and 500 m water depth. The seabed where these deposits outcrop often has relict iceberg pits and scours (Figure 9). The acoustically incoherent material is interpreted to be till, and elsewhere on the upper slope, till slabs and terraces are imaged in huntec data (Brunt et al., 2004). Cores from the area recover little sediment (Figure 10) and shear strength measurements indicate stiff material.

Proglacial mud

Proglacial mud consists of acoustically stratified mud (Figure 11) with interbedded sand and mud layers and sparse ice-rafted debris, formed through deposition from meltwater plumes interspersed with deposition from turbidity currents. It occurs on intercanyon ridges in water depths typically <1500 m. Cores from intercanyon ridges have a stratigraphy that is correlateable from ridge to ridge (Jenner et al., in press) and show normal increases in bulk density and shear strength (Figure 12).

Canyon and channel fill deposits

Canyon and channel fill deposits consist of acoustically incoherent alternating mass transport deposits and mud to gravelly-sandy mud occurring in channels and canyon floors. In canyon floors a transition from higher to lower values of acoustic backscatter, derived from the multibeam data, occurs at ~1000 m water depth and is interpreted to represent the transition from sandy canyon floor to muddy canyon floor. Cores from this area have a muddy drape at the top of the core, with an unconformity over stiffer material several centimetres to metres downcore (Figure 13). Sub-bottom profiles from canyon floors are generally incoherent, partially a result of the geology, but also a result of side echoes from nearby steep canyon walls (Figure 14).

Fine to medium sand

A centimetre to metre thick layer of fine to medium sand deposited by resuspension and advection from the shelf during storms and sandy turbidity flows. It occurs at the heads of most canyons and in the thalweg of major canyons. Canyon floors on the upper slope have high acoustic backscatter interpreted to represent sandy sediment on the seabed. Cores from this area contain sand and sandy silt (Figure 15). Sub-bottom profiles show acoustically stratified sediments over incoherent sediments (Figure 16).

Sand or gravelly sand

A >1m thick layer of sand or gravelly sand, deposited during the late Pleistocene and early Holocene and reworked by major storms. It occurs on the upper slope between 100 m and 300 m water depth and typically overlies ice-margin sediments. Sub-bottom data from smooth areas of the outer shelf show thin stratified deposits over acoustically incoherent deposits interpreted as till draped with sand or gravelly sand (Figure 17).

Seabed Topography Along Route Scenarios

A series of graphs were prepared for each route scenario. The graphs show for each route the surficial geology, bathymetry, gradient, as well as the median gradient and standard deviation within a 200 m corridor.

Route 1: Straight line- Annapolis field to outer shelf

Route 1 traverses from the Annapolis field to the outer shelf in a straight line. As a result, it is the most variable route in terms of seabed relief and surficial geology (Figure 18, Figure 19a). The shelf break occurs at ~400 m water depth and coincides with a transition from ice-margin deposits to canyon head deposits. Bathymetry along the slope portion of the route is variable because the route intersects a number of canyons and intercanyon ridges. The maximum gradient along the route is 47° with prolonged intervals with gradients >20° corresponding to canyon walls. The standard deviation within the corridor is as high 13°, indicating that the seabed gradient is quite variable in some areas. The greatest amount of variability occurs in canyon walls and in canyon heads.

Route 2: Intercanyon ridge- Annapolis field to the outer shelf

Route 2 traverses from the Annapolis field to the outer shelf along an intercanyon ridge (Figure 19a, Figure 20). The shelf break is gradual along the route, occurring at ~300 m within ice-margin deposits. The general shape of the slope along the route is convex, on which smaller scale undulations are superimposed. The maximum gradient along the route is 35°, at a small scarp on a muddy ridge. The median gradient within the 200 m corridor is generally less than 15°, with higher spikes correlating to escarpments on the muddy intercanyon ridge. The standard deviation is typically less than 5° except at escarpments, where it is as high as 11° and the gradient is more variable.

Route 3: Canyon floor- Annapolis field to the outer shelf

Route 3 traverses from the Annapolis field down a canyon wall and then up a canyon floor to the outer shelf (Figure 19a, Figure 21). The shelf break occurs at 400 m water depth at the transition from ice-margin deposits to canyon head deposits. The general shape of the canyon floor along the route is concave. The maximum gradient along the route is 49° and occurs down the canyon wall. The maximum gradient within

the canyon floor is 26° and is due to a small escarpment, whereas typical gradients within the canyon floor are less than 12°. The median gradient with in the 200 m corridor is generally less than 10°, with higher spikes correlating to escarpments within the canyon floor and the canyon wall. Standard deviation is as high as 13° on the canyon wall, but is typically less than 5°.

Route 4: Intercanyon ridge- Arbitrary location to the outer shelf

Route 4 traverses from the arbitrary location along a particularly sharp-crested intercanyon ridge to the outer shelf (Figure 19b, Figure 22). The shelf break is gradual along this route and occurs within ice-margin deposits between 300 and 500 m water depth. The general shape of the seafloor along the route is convex with gentle undulations. The maximum gradient along the route is 42° and occurs within proglacial mud on an intercanyon ridge. There are a number of high gradient spikes along this route which occur along the ridge and are due to the sharp crested morphology of the ridge and the steepness of the adjacent canyon walls. The median gradient within the 200 m corridor is high, generally greater than 15°. Again, this appears to be a result of the sharp crested shape of the ridge, resulting in the corridor encompassing both ridge crest and canyon wall areas. Typically, the standard deviation is between 5° and 10°.

Route 5: Canyon floor: Arbitrary location to the outer shelf

Route 5 traverses from the arbitrary location up a canyon floor to the outer shelf (Figure 19b, Figure 23). The shelf break occurs at ~400 m water depth within ice-margin deposits. The shape of the seafloor along this route is concave up with very few small scale variations. The maximum gradient along the route is 42°, but appears to be associated with a data artefact. Typically the gradient along the route is less than 10° except for the upper slope where it is between 10° and 20°. The median gradient along the 200 m corridor is similar to the actual gradient and is reflected in the low standard deviation.

Sediment Mobility and Currents

An assessment of sediment transport should be considered in a geohazard evaluation for submarine pipeline routes (DNV, 2004). This can be done through direct measurements of storm wave heights and ocean currents, seafloor observations, as well as examination of evidence in the geological record. This section provides a review of storm driven currents, tidal currents, turbidity currents, sediment mobility and failure risk on the Scotian Slope.

Current meter observations

The Ocean Sciences Division (OSD) at the Bedford Institute of Oceanography maintains a database of near bottom current measurements on the east coast (http://www.mar.dfo-mpo.gc.ca/science/ocean/current_statistics/BottomCurrents.html). These data report current meter measurements taken within 10 m of the seafloor, with the deepest measurements taken at a water depth of 729 m. In water depths between 500 m and 729 m, maximum velocities measured exceed 0.90 m/s. The OSD also provide summaries of all other current meter measurements from the Atlantic margin (http://www.mar.dfo-mpo.gc.ca/science/ocean/database/data_query.html). As an experiment, all the measurements from the Scotian Slope within 150 m of the seafloor were extracted. This resulted in 25 locations and 154 measurements from water depths ranging from 85-3500 m (Figure 24). For the deepwater areas (beyond 500 m water depth), current velocities were as high as 0.95 m/s, but typically ranged from 0.15-0.40 m/s (Figure 25).

Storm driven currents

Storm driven currents can mobilize sediment in water depths up to 200 m or more. In the western Atlantic, wave heights of over 30 m (the highest ever measured) have been recorded since the late 1980's (Swail, 1997). There have been no direct observations of storm effects on sediment mobility on the Scotian Slope, however there is a planned RALPH deployment at the head of Logan Canyon for the summer of 2005.

Geological studies in the vicinity of the Albatross and Shelburne exploration wells have shown the effect of large storms on transport of sand on the continental slope. Sorted sands and silts, apparently derived from the outer continental shelf and remobilised by storm-driven currents, mantle the upper slope to water depths of 450-600 m (Hill and Bowen, 1983) and occur in mid-slope channels (Baltzer et al., 1994). A core from near Logan Canyon in 920 m water depth (87003-007) was analysed for a storminess record using weight percent sand as a proxy for storminess (Campbell, 1999). The core showed two major increases in sediment reworking, one interval that is well dated and appears to coincide with the Younger Dryas cooling event, and another interval near the top of the core, the base of which appears to coincide with the Little Ice Age.

Tidal currents

Deepwater tidal currents, recognised by semi-diurnal peaks in velocity in current meter studies, have been recognised for some time. However, the effects of these currents on sediment mobility and sediment deposition is not yet well understood (Shanmugan, 2003). Submarine canyons have unique morphology which serves to focus tidal energy, resulting in a funnelling effect. Shepard et al. (1979) reported current velocity measurements within canyons from various water depths by suspending current meters 3 metres off the seafloor. Their results show that tidal currents ranged from 0.19-0.39 m/s during up-canyon flow and 0.13-0.52 m/s during down-canyon flow.

Turbidity currents

There is abundant geological evidence for past turbidity current activity on the Scotian Slope found in cores, seismic reflection profiles and surficial morphology (Mosher et al., 2004). Cores have been found to contain sparse gravel beds, sand laminae and beds, as well as mud/silt laminasets. Many of the deposits are of Pleistocene age and are probably a result of either failure of proglacial sediments in canyon heads or direct hyperpycnal flow from subglacial meltwater at an ice margin. Evidence of recent turbidity currents is less abundant. During the Holocene, turbidity flows are probably restricted to thalweg channels in major canyons (Verrill, Dawson, Logan, the Gully) (Figure 2). These flows could be generated by different processes. Sediment can be put

into suspension on the shelf during major storms which then evolve into turbidity currents at canyon heads. There is seismic evidence of sand prograding towards canyon heads in some parts of the Scotian Slope (Figure 6) which may fail occasionally down the canyon resulting in a turbidity current. The 1929 Grand Banks turbidity current, which broke several submarine communications cables, was triggered by a M7.2 earthquake and subsequent landslide.

Recent sediment mobility and seabed failure

Evidence of Holocene sediment mobility on the slope is less abundant than evidence from the Pleistocene. A few major canyons, namely Verrill, Dawson, Logan and the Gully, indent the outer shelf and have a narrow thalweg which presumably are conduits for occasional flows down the canyon (Figure 2). Sand beds have been imaged in subbottom profiler data that appear to be prograding towards canyon heads near Logan Canyon. On the upper slope west of Verrill Canyon, a zone bedforms is apparent in multibeam bathymetry (Figure 26). These bedforms have relief of ~2 m, wavelengths of ~150 m and are confined to water depths of 200-250 m. It is not clear what processes are involved in the formation of the features, but they may be formed by an internal tide or internal wave phenomenon.

Failures within the Holocene section on the Scotian margin appear to be rare. The best studied is the 1929 failure which was earthquake triggered and described in detail by several authors (Piper et al., 1999, Hughes-Clarke et al., 1990, Hughes-Clarke et al., 1989 and others). The earthquake magnitude was high (7.2) and failure was recognised as much as 100 km from the epicentre. Jenner et al (in press) show that within the vicinity of Logan Canyon, two localised Holocene failure events are recognizable from core samples. These failures appear to be synchronous and occur across different canyon systems, which would suggest a regional trigger such as an earthquake. Radiocarbon dating from the samples indicate that the first event occurred around 7 ka and the second event occurred around 1 ka. The failures are not recognizable in sub-bottom profiles and are not believed to be the same magnitude as the events that occurred during either the late Pleistocene or triggered by the 1929 earthquake.

Seismic Activity

Large earthquakes are rare off eastern Canada. There have been 3 earthquakes recorded since 1927 within 100 km of the study area (NEDB, 2003); a M 3 in 1927, a M 3.2 in 1989, and a M 2.3 in 2002 (Figure 27). Mosher et al. (1994) demonstrated using infinite slope stability analysis that the upper 25 m of sediment on the slope is stable under static conditions. In 1929 a M 7.2 earthquake occurred ~320 km east of the study area on the continental slope that triggered a major submarine landslide which damaged communications cables that were in the path of the slump and turbidity flow (Piper et al. 1999). On January 25, 2005, a M4.7 earthquake was recorded within the vicinity of the 1929 event (NEDB, 2005).

Discussion

Appropriate pipeline route selection requires avoidance of geohazards both during installation and operation, while at the same time selecting the shortest route possible in order to keep material costs down. A straight line route scenario will often appear to be the most economic option since it uses the least amount of materials. In fact, most pipeline routes start as linear and are then modified along the route to avoid any hazards, or to avoid expensive installation procedures such as trenching, or to follow a natural feature such as a channel. In this study, three types of routes were examined: a) a strictly linear route, b) a route that followed an intercanyon ridge, and c) a route that followed a canyon floor.

During pipeline installation, the biggest risk is associated with factors that may lead to pipeline buckling (Carr and Preston, 1999). In the Logan Canyon area, the factor that would have the greatest impact on pipeline route selection is the severe topography associated with the canyoned terrain. In every route scenario examined, there are sections where median slope angles exceed 15° for up to a kilometre or more, and locally there are intervals where slope angles exceed 30°. It was obvious from the route analysis that the straight line scenario for the Annapolis field was least favourable in terms of severe terrain. The straight line scenario crossed two canyon walls which is where the

steepest slope angles are encountered. Depending on the location of the field, it may be impossible to avoid traversing canyon walls with a pipeline. For example, for the canyon floor scenario at the Annapolis field, the pipeline would first have to move laterally down a canyon wall before entering the canyon floor (Figure 2). Similarly for the intercanyon ridge scenario at the arbitrary location, the pipeline would have to go up the canyon wall before getting to the intercanyon ridge (Figure 2). Once the pipeline is positioned within either the canyon or on top of the ridge, the topography becomes much more benign, at least at the scale of the available bathymetric data.

Sediment instability can lead to pipeline buckling during installation. Again the objective is to avoid steep, unconsolidated slopes which may become unstable during installation. This may be difficult in some areas, for example along a particularly sharp ridge crest. In these areas, the crest of the ridge can be less than 100 m wide (fig ridge crest) and the slopes adjacent to the crest are quite steep. The ridge crest sediments comprise mainly hemipelagic muds which are weak and may be prone to failure if disturbed. There are places along the canyon floor routes where the canyon floor becomes less than 250 m wide with adjacent steep canyon walls. Canyon walls are generally thought to comprise competent material based on sampling experience and observation (broken sampling equipment, recovery of overconsolidated sediment, observation of outcropping strata), but locally may be draped by several metres of unconsolidated sediment.

Other geological constraints to consider during installation are deposits that may inhibit trenching. On the outer shelf, there is an area of seabed which is heavily pitted and scoured by icebergs. These are relict features formed at the end of the Pleistocene during a period of lower sea-level. Much of the sediment below this type of seabed comprises diamict (probably glacial till) which is overconsolidated and consists of a poorly sorted mixture of stiff mud, gravel, and occasional large boulders. As well, canyon floors can contain apparently overconsolidated material such as sediment blocks derived from canyon walls during erosive flows, sand and gravel beds. Finally, the composition of the top few metres of sediment on canyon walls is variable, ranging from normally consolidated Holocene muds to lithified outcropping strata, which makes it

difficult to predict foundations conditions at a particular location without a detailed site survey.

During operation, a number of other factors would need to be considered. Gravitational stress on the pipeline due to steep slopes, which in areas can exceed 45°, must be taken into account. Sediment failures in the study area appear to be rare, with only a few events recognized during the Holocene (Jenner, et al., in press). The likelihood that a landslide would occur within the study area due to natural processes and impact a pipeline during the lifetime of the structure is very low (Piper and Normark, 1982) (Piper et al., 2003). However, the local impact of loading effects on seafloor stability, due to the weight of the pipeline and associated infrastructure, should be considered. The frequency of turbidity flows and other erosive flows down canyons also appears to be low based on the low sedimentation rates during the Holocene compared to the Pleistocene. That said, a number of canyons which indent the outer shelf appear to have active thalwegs formed by occasional flows. A proposed RALPH deployment at the head of Logan Canyon in the summer of 2005 will hopefully give some insight into the sediment dynamics at the heads of large canyons.

Conclusions

Five deepwater pipeline scenarios were investigated for the Scotian Slope. The purpose of the investigation was to assess geological constraints to pipeline placement in a deepwater environment. The study area was chosen because of its proximity to existing hydrocarbon infrastructure on the shelf (Sable Gas Project) and the location of a recent gas discovery on the slope near Logan Canyon. It is an area of severe topography, with canyon walls exceeding 45° in places. It is also an area of variable surficial geology, ranging from unconsolidated muds on intercanyon ridges, to outcropping strata on canyon walls, to bouldery diamict on the upper slope. There is little evidence of sediment instability during the Holocene in the area, but there is evidence of active sediment transport down canyons and at canyon heads. Detailed, site-specific investigations would have to be conducted before any infrastructure was put in place.

Acknowledgements

This work was conducted under the offshore geohazards project of the Geoscience for Ocean Management Program and is a contribution to the Program for Energy R&D project 532211. This report was improved through discussions with David J.W. Piper.

References

Brunt, R, Piper, D.J.W., and Campbell, D. C. 2004. Compilation of surficial geological data from the upper Scotian Slope (150 to 500 metres below sea level). Geological Survey of Canada, Open File 4622, 15 pages plus 1 CD.

Campbell, D.C., 1999. Holocene storminess on the Scotian Shelf: the last 7000 years. Unpublished B.Sc. honours thesis, Saint Mary's University. 92 pages.

Carr, P. and Preston, R. 1999. Risk Assessment of Deepwater Gas Trunklines. 2nd International Deepwater Pipeline Technology Conference, March 1999, 24 p.

DNV (Det Norske Veritas) 2004. Offshore Standard DNV-OS-F101 Submarine Pipeline Systems. Det Norske Veritas, Norway, 166 p.

Driscoll, A.H., K. Moran, D.J.W. Piper, and G. Vilks, 1989, An improved deep coring system. Offshore Technology Conference, Houston, Texas, Paper OTC 5962.

Henriksson, A., Wilhelmsen, A., and Karlsen, T. 2004. Pipelines in harsh environments. Offshore Technology Conference, Houston, Texas, Paper OTC 16557.

Hill, P.R. and Bowen, A.J. 1983. Modern sediment dynamics at the shelf slope boundary off Nova Scotia; in The Shelfbreak. Critical Interface on Continental Margins, eds. D.J. Stanley and G.T. Moore; Society of Economic Palaeontologists and Mineralogists Special Publication No. 33, p. 265-276.

Hughes Clarke, J.E., Mayer, L.A., Piper, D.J.W. and Shor, A.N., 1989. Pisces IV submersible operations in the epicentral region of the 1929 Grand Banks earthquake. Geological Survey of Canada Paper 88-20, p. 57-69.

Hughes Clarke, J.E., Shor, A.N., Piper, D.J.W. and Mayer, L.A., 1990. Large scale current-induced erosion and deposition in the path of the 1929 Grand Banks turbidity current. Sedimentology, v. 37, p. 613-629.

Jenner, K.A., Piper, D.J.W., Campbell, D.C. and Mosher, D.C., 2005. Lithofacies and origin of late Quaternary mass transport deposits in submarine canyons, centr Scotian Slope, Canada. Sedimentology (in press).

Marshall, R. and McDonald, W. 2004. Mardi Gras transportation system overview. Offshore Technology Conference, Houston, Texas, Paper OTC 16637.

McCoy, J. and Johnston, K. 2001. Using ArcGIS Spatial Analyst. Environmental Systems Research Institute, Inc. 230 pages.

Mosher, D.C. 2000. CCGS Hudson Expedition 2000-042. Geological Survey of Canada cruise report.

Mosher, D.C., Piper, D.J.W., Campbell, D.C., and Jenner, K.A. 2004. Near surface geology and sediment failure geohazards of the central Scotian Slope. AAPG Bulletin, v. 88, p. 703-723.

Piper, D.J.W. and Campbell, D.C. 2002. Surficial geology of the Scotian Slope, Eastern Canada: Geological Survey of Canada Current Research 2002-E15, 10 p.

Piper, D.J.W., Mosher, D.C., Gauley, B.J., Jenner, K. and Campbell, D.C. 2003. The chronology and recurrence of submarine mass movements on the continental slope off southeastern Canada. In: Locat, J. and Mienert, J., Submarine mass movements and their consequences. Kluwer, Dordrecht, p. 299-306.

Piper, D.J.W. and W.R. Normark, 1982, Effects of the 1929 Grand Banks earthquake on the continental slope off eastern Canada: Geological Survey of Canada Paper 82 1B, p. 147 151.

Piper, D.J.W., Cochonat, P., and Morrison, M.L. 1999. The sequence of events around the epicentre of the 1929 Grand Banks earthquake: Initiation of the debris flows and turbidity current inferred from sidescan sonar: Sedimentology, v. 46, p. 79-97.

Shanmugam, G. 2003. Deep-marine tidal bottom currents and their reworked sands in modern and ancient submarine canyons. Marine and Petroleum Geology, v. 20, p. 471-491.

Shepard, F.P., Marshall, N.F., McLoughlin, P.A., and Sullivan, G.G. 1979. Currents in submarine canyons and other sea valleys. AAPG Studies in Geology No. 8. Tulsa, Oklahoma, 173 p.

Swail, V. 1997. Ocean Waves. In Climate Change and Climate Variability in Atlantic Canada:Volume VI of the Canada Country Study: Climate Impacts and Adaptation. Edited by J. Abraham, T. Canavan, and R. Shaw. Environment Canada. pp. 27- 31.

Tootill, N.P., Vandenbossche, M.P. and Morrison, M.L. 2004. Advances in deepwater pipeline route selection- A Gulf of Mexico case study. Offshore Technology Conference, Houston, Texas, Paper OTC 16633.

World Wide Web references:

NEDB (National Earthquake Database), accessed December 2003. url: http://seismo.nrcan.gc.ca/nedb/index_e.php

NEDB (National Earthquake Database), accessed June 2005. url: http://seismo.nrcan.gc.ca/nedb/index_e.php

OSD (Ocean Sciences Division, Dept. of Fisheries and Oceans), archive of near bottom currents, accessed June 2005. url: http://www.mar.dfo-mpo.gc.ca/science/ocean/current_statistics/BottomCurrents.html

OSD (Ocean Sciences Division, Dept. of Fisheries and Oceans), Oceanographic Databases, accessed June 2005. url: http://www.mar.dfo-mpo.gc.ca/science/ocean/database/data_query.html

Figures

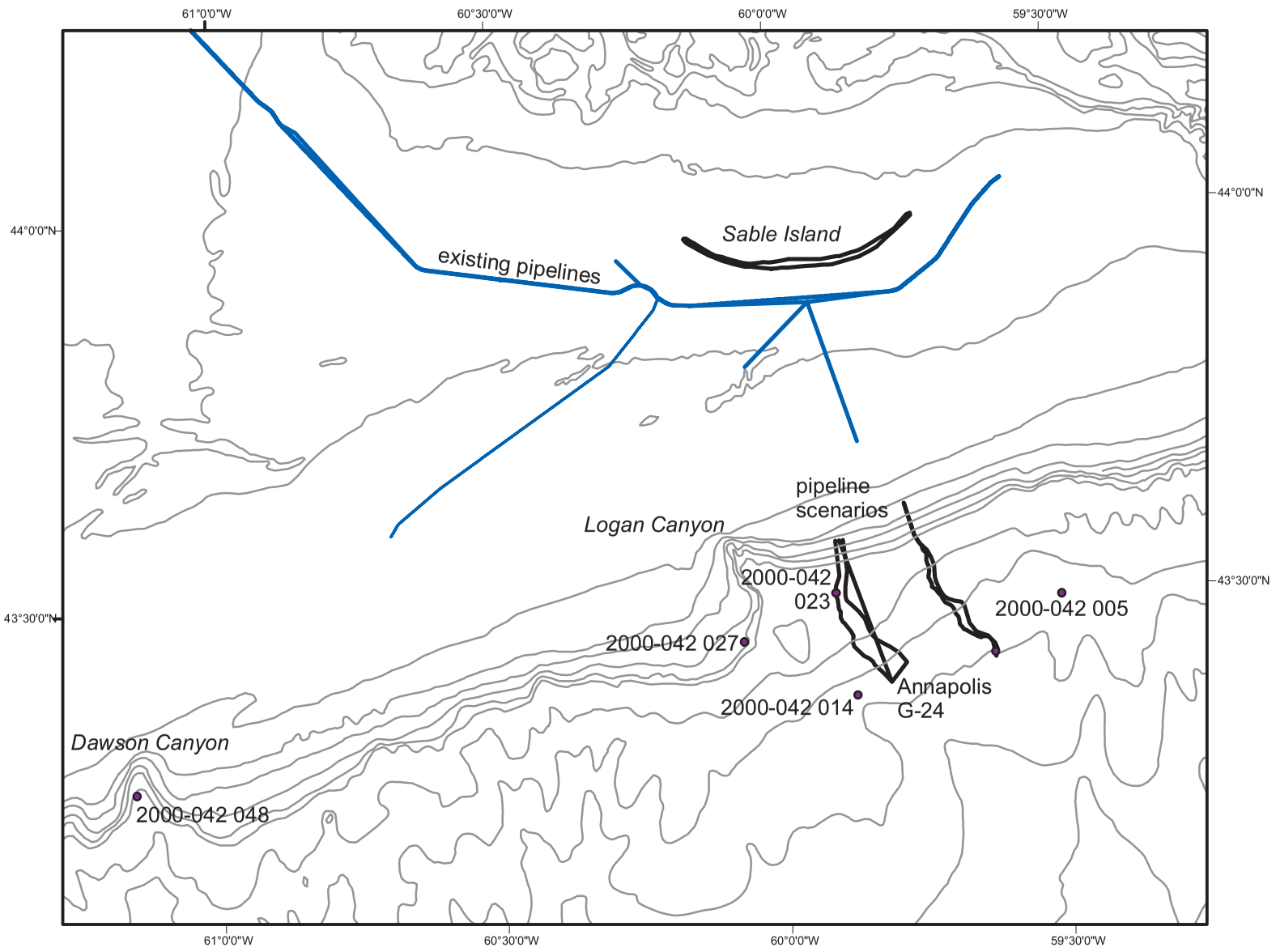

Figure 1: Overview of the existing infrastructure, location of pipeline scenarios and piston cores used in this study.

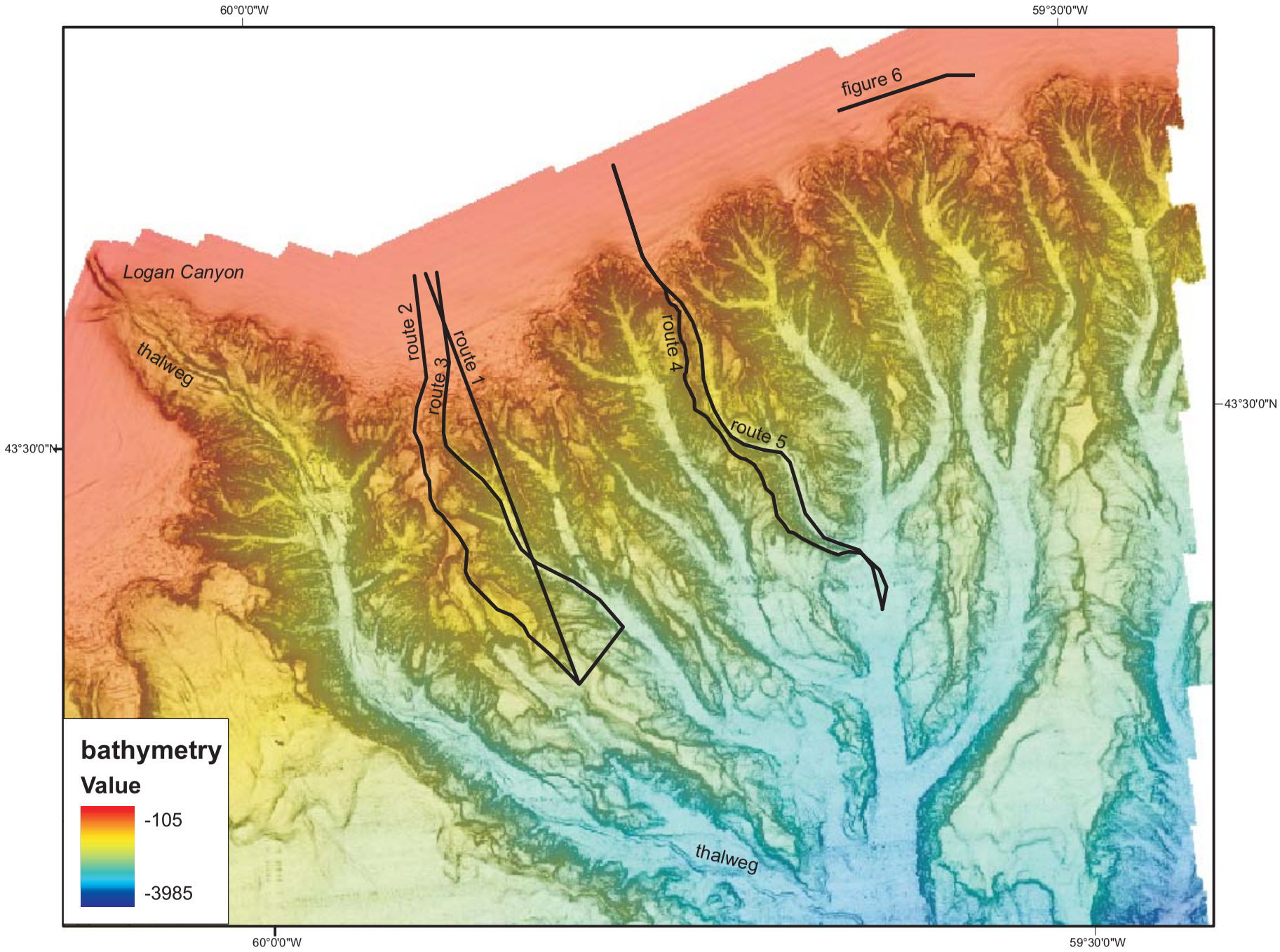

Figure 2: Location of route scenarios for this study. Background is a DTM of the study area overlain with a gradient surface (shallow slopes are white, steep slopes are black).

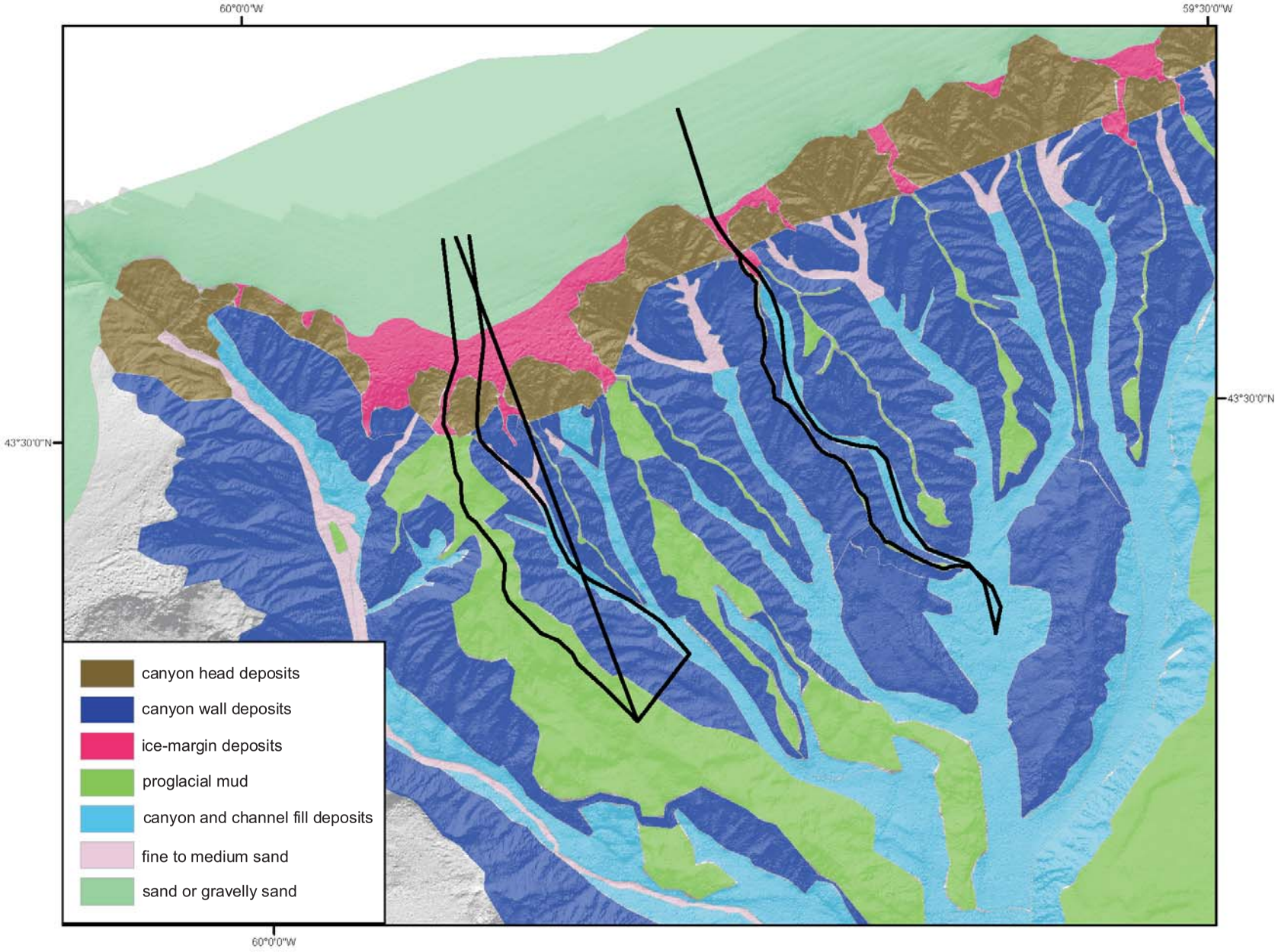

Figure 3: Surficial geology of the study area.

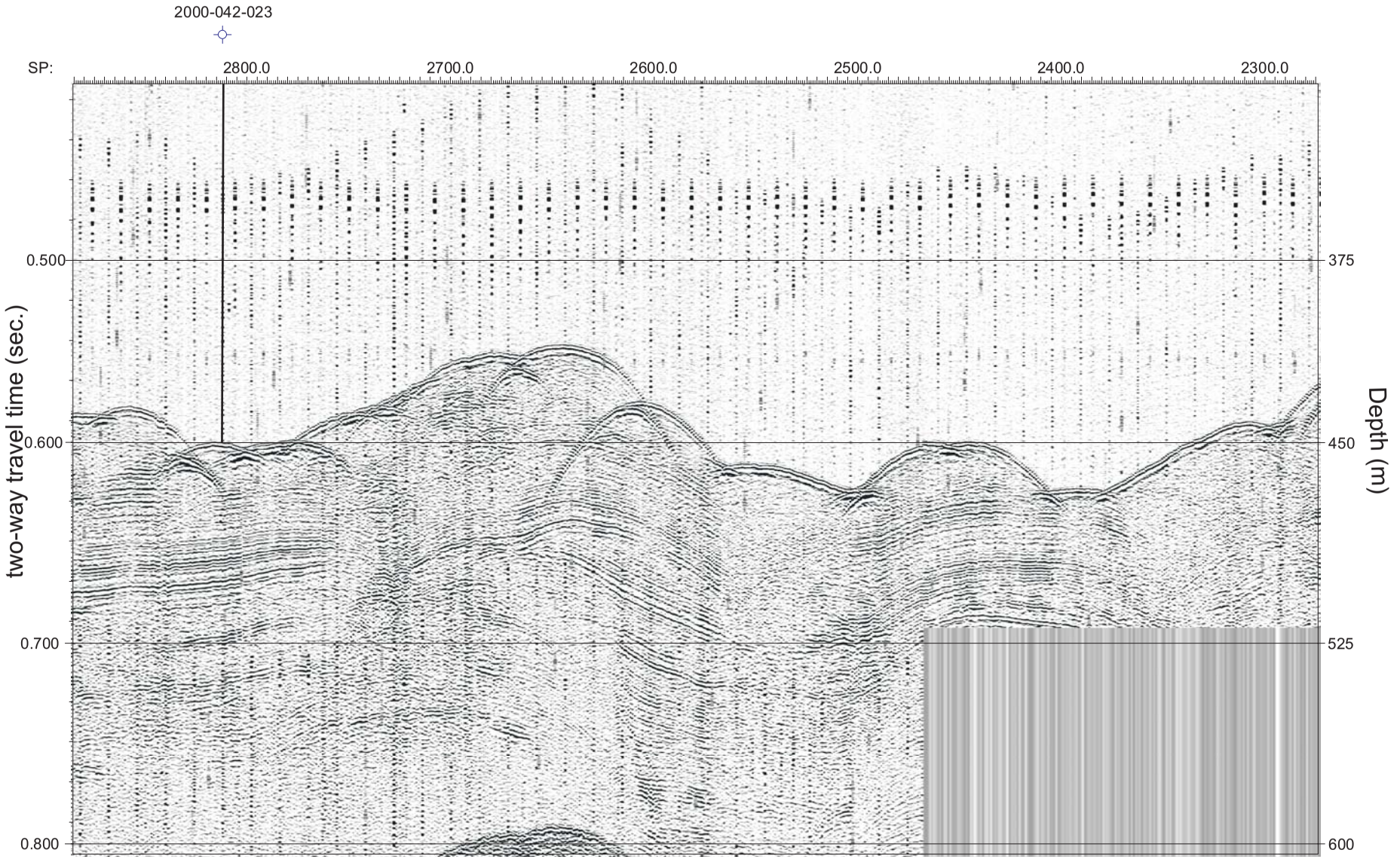

Figure 4: Huntec seismic reflection profile at a canyon head showing core site 2000-042 023. See figure 1 for location of core site.

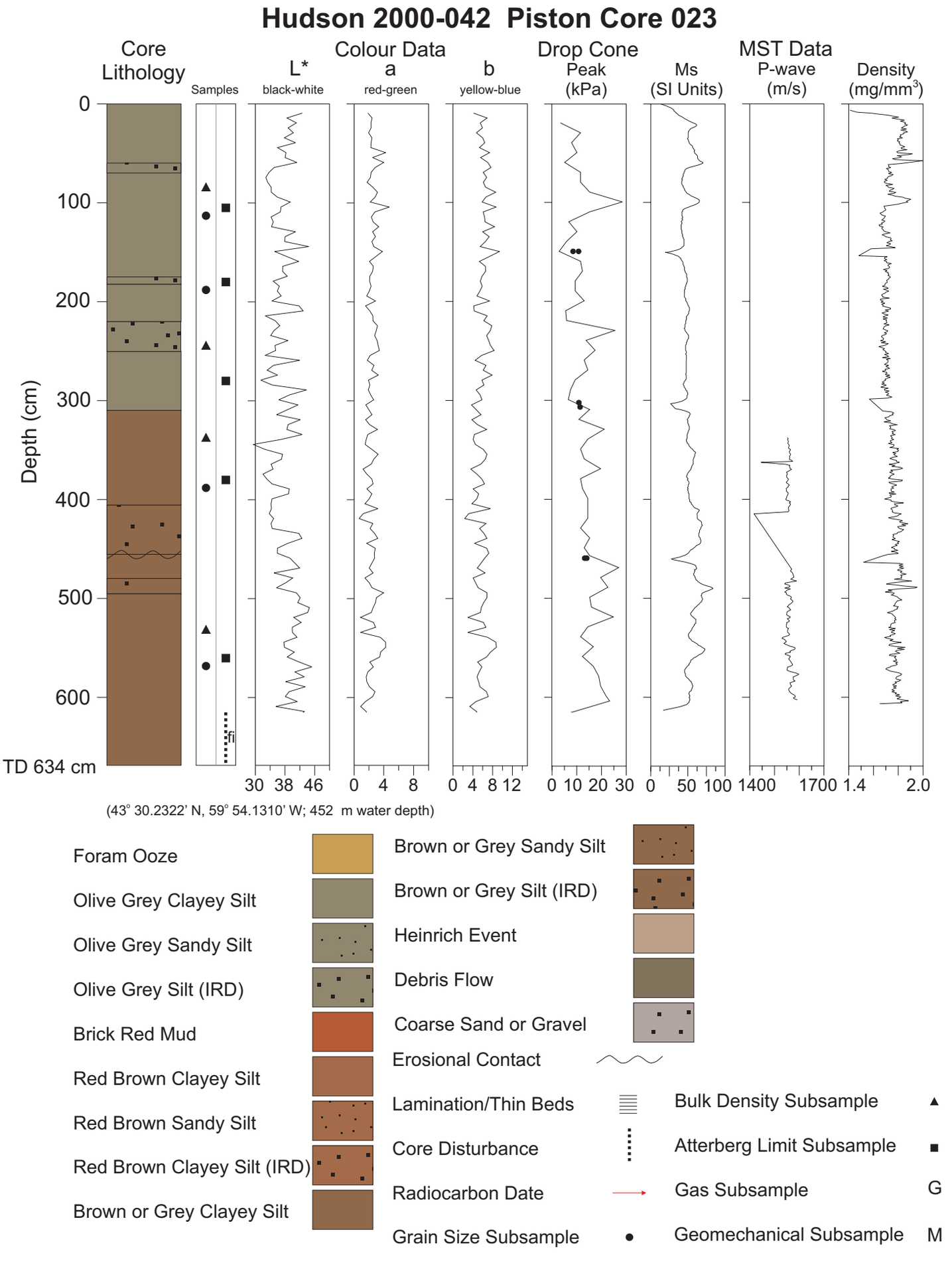

Figure 5: Downcore lithological and physical properties plot for core 2000-042 023 taken at a canyon head.

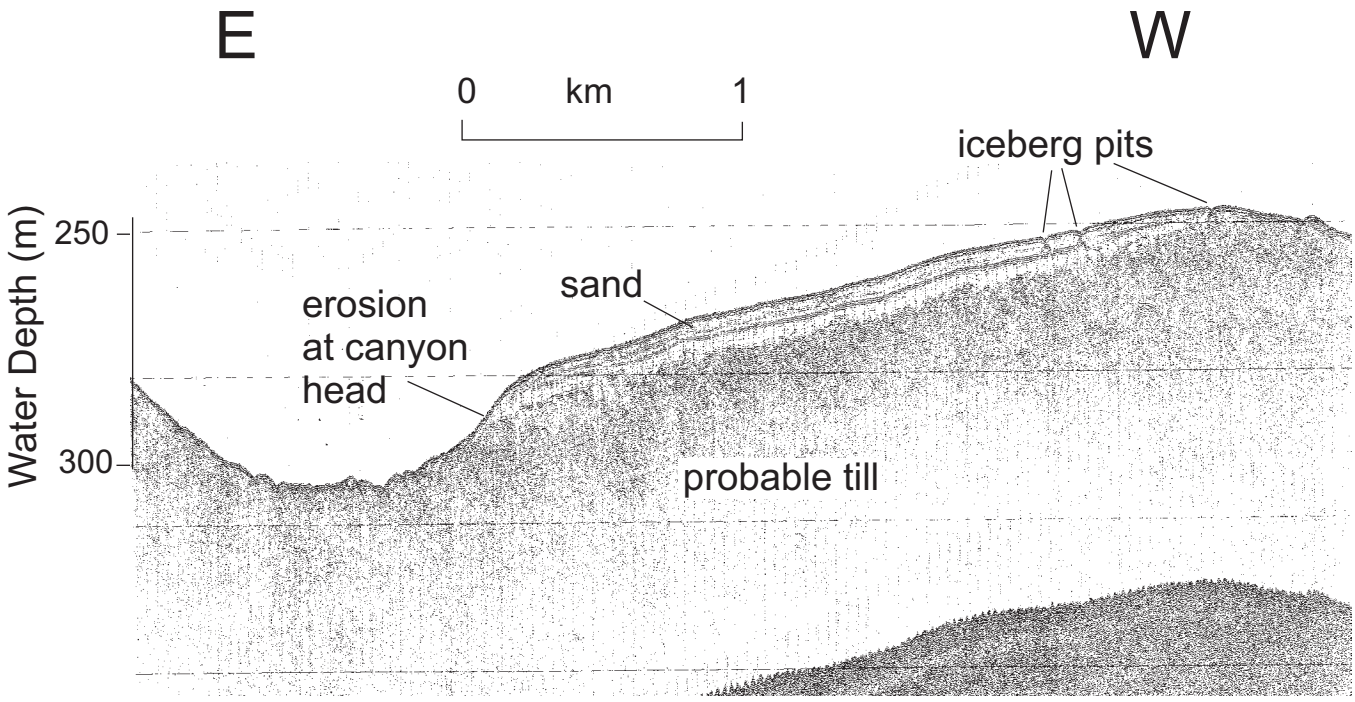

Figure 6: Huntec seismic reflection profile at the head of a canyon showing sand progradation and erosion (modified from Piper and Campbell (2002)). See figure 2 for location.

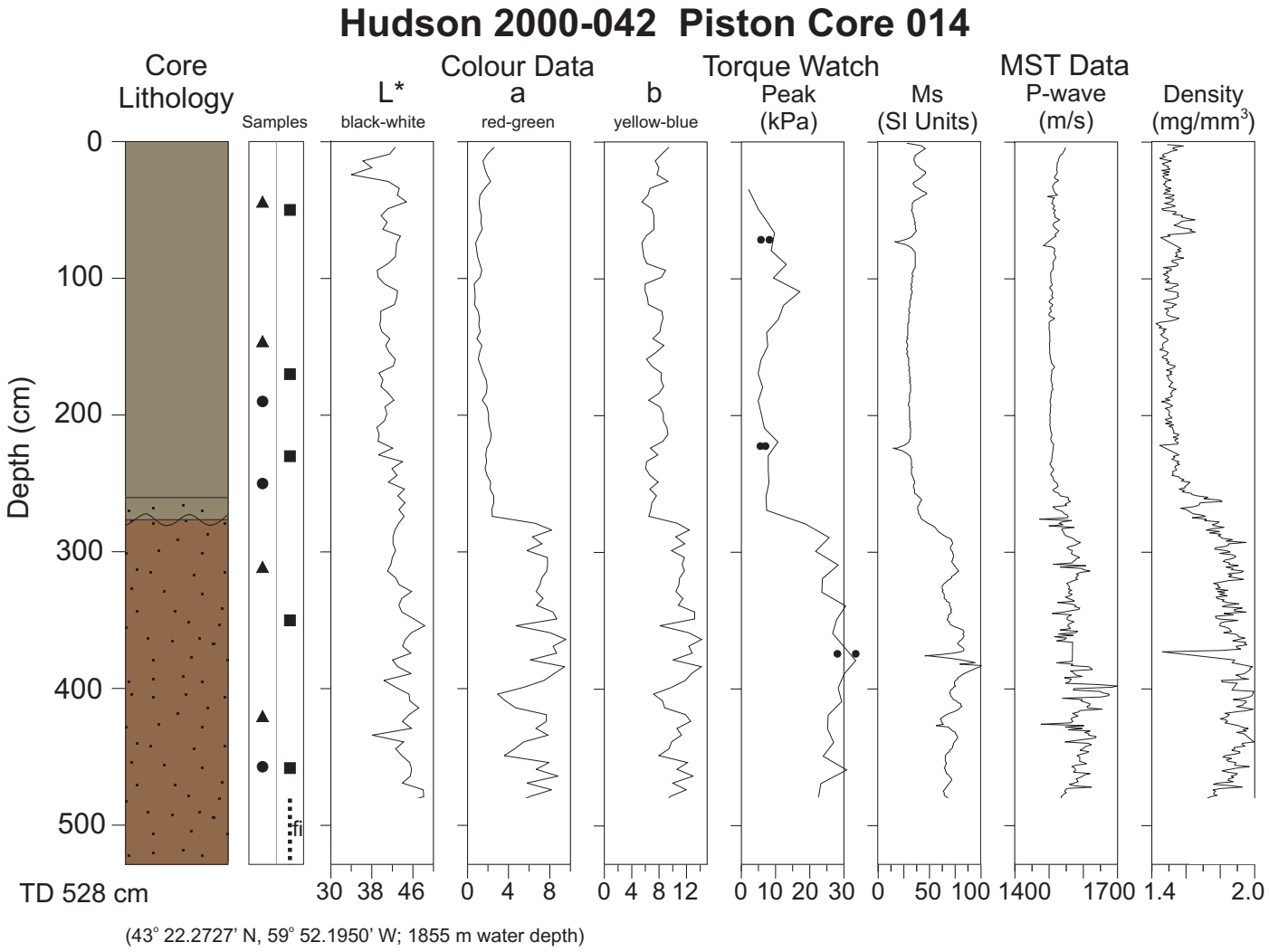

Figure 7: Downcore lithological and physical properties plot for core 2000-042 014 taken from a canyon wall. See figure 5 for legend and figure 1 for core location.

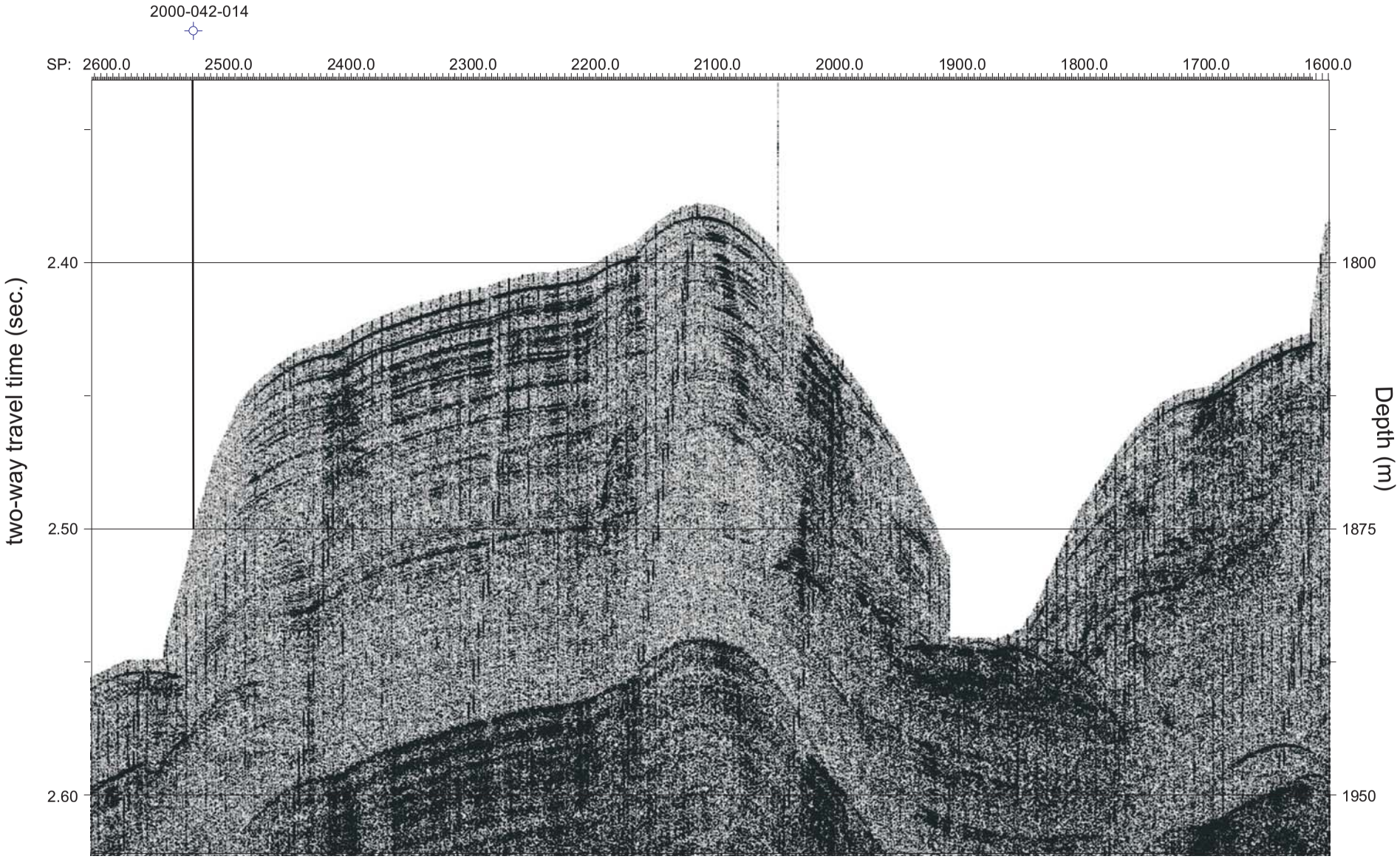

Figure 8: Huntec seismic reflection profile from a canyon wall showing core site 2000-042 014. See figure 1 for location of core site.

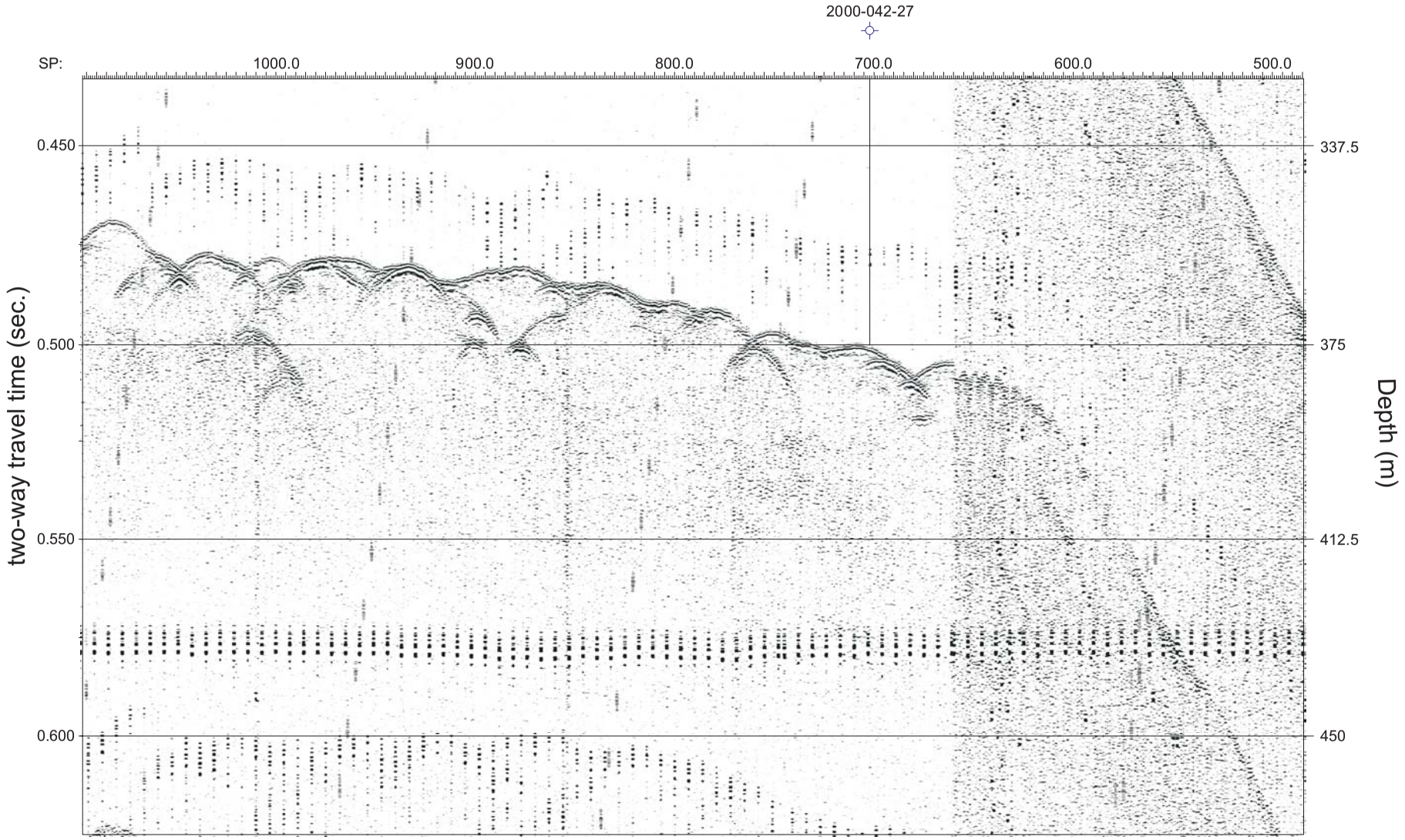

Figure 9: Huntec seismic reflection profile from an area of outcropping ice-margin deposit showing core site 2000-042 027. See figure 1 for location of core site.

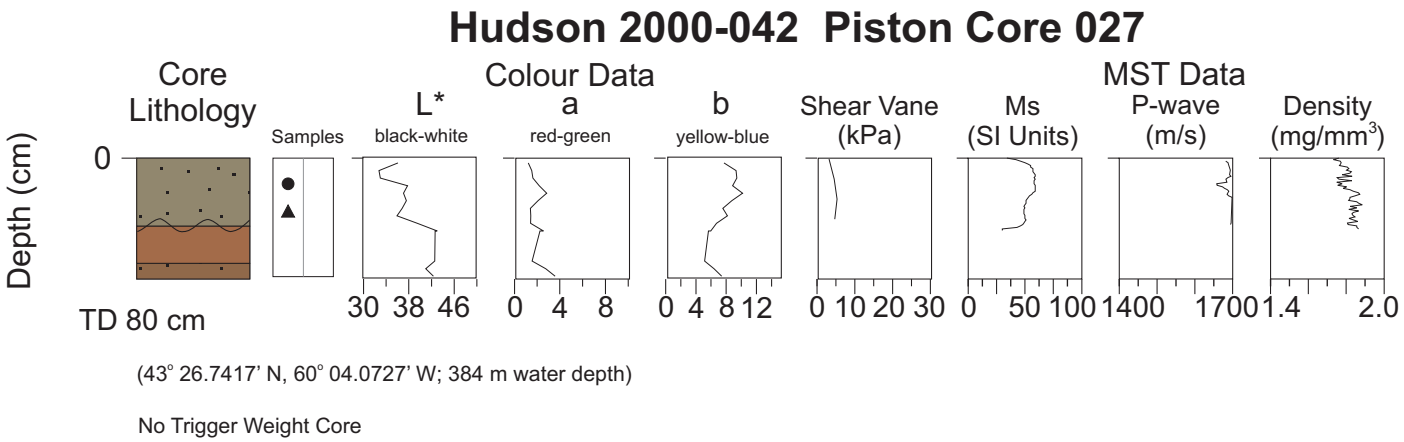

Figure 10: Downcore lithological and physical properties plot for core 2000-042 027 taken in ice-margin deposits. See figure 5 for legend and figure 1 for core location.

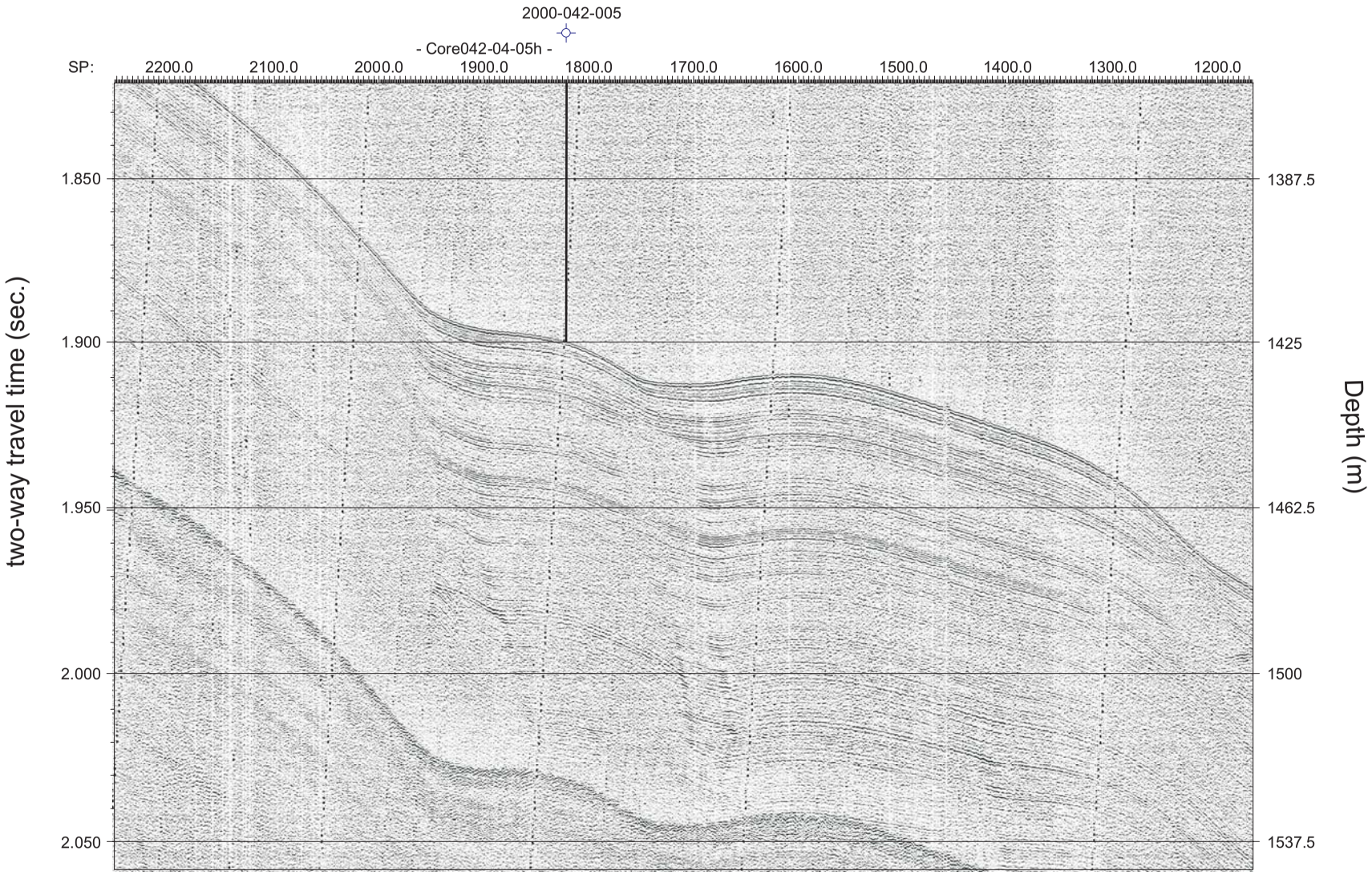

Figure 11: Huntec seismic reflection profile from a muddy ridge showing core site 2000-042 005. See figure 1 for location of core site.

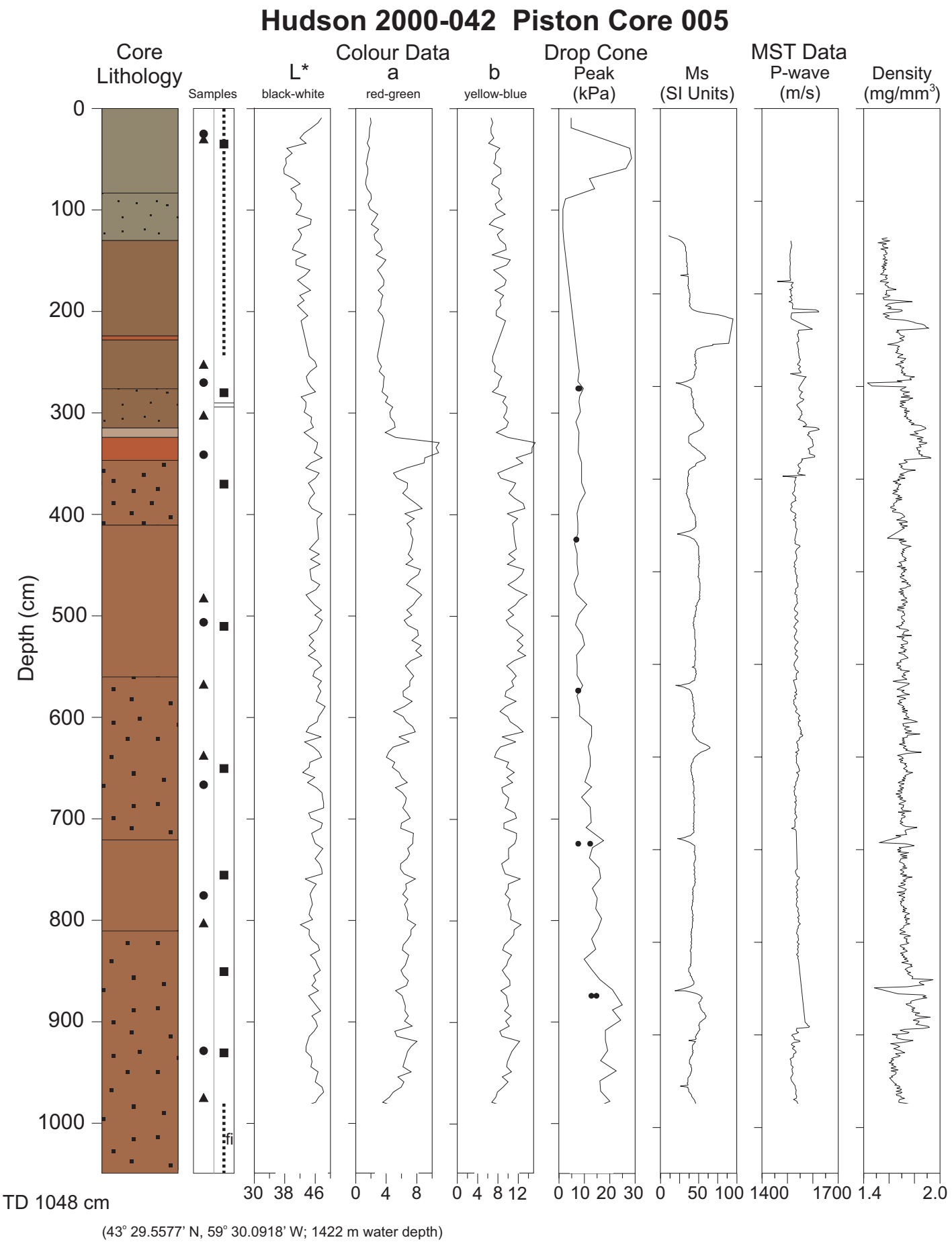

Figure 12: Downcore lithological and physical properties plot for core 2000-042 005 taken in proglacial mud on a ridge. See figure 5 for legend and figure 1 for core location.

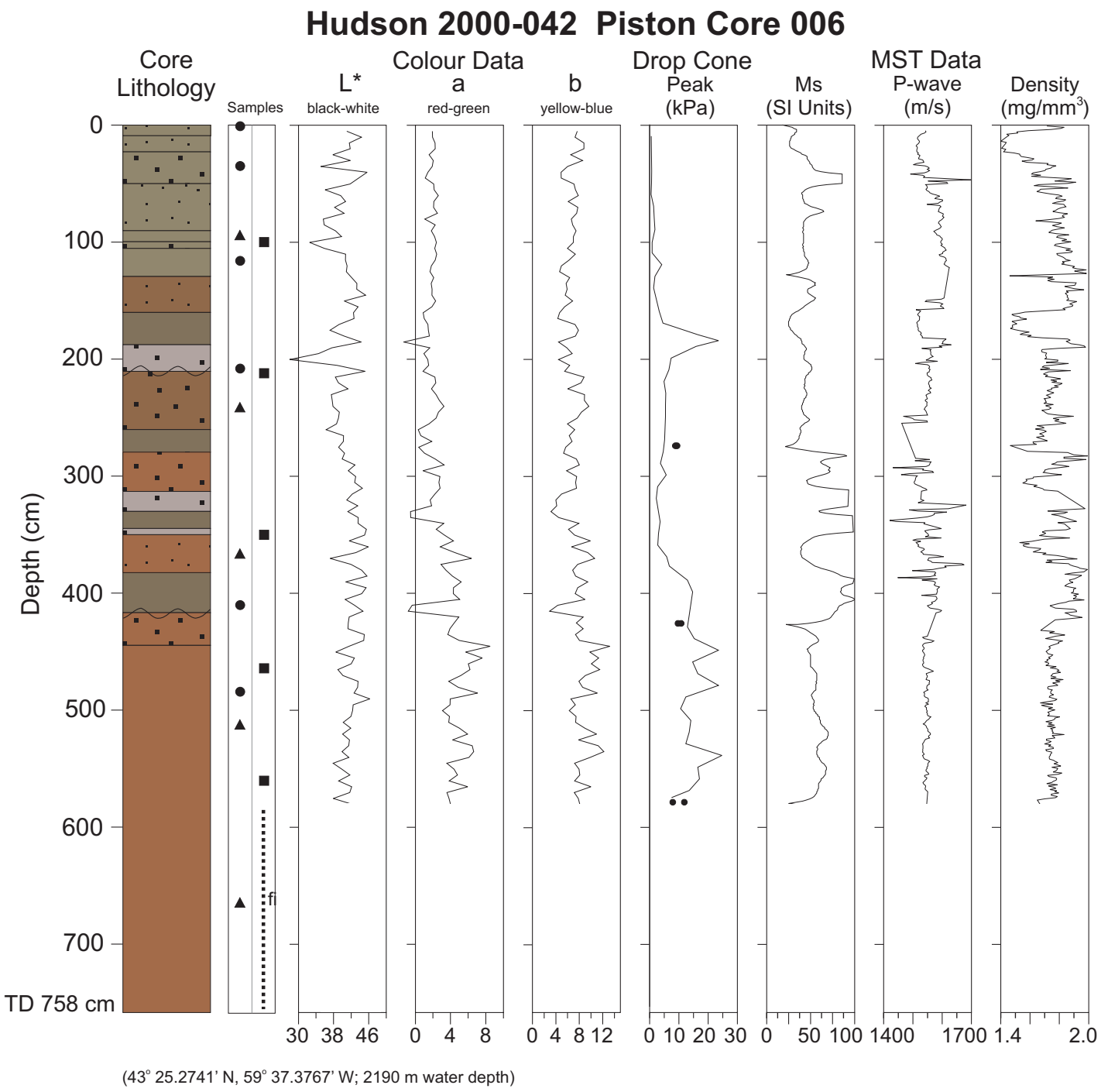

Figure 13: Downcore lithological and physical properties plot for core 2000-042 006 taken from a muddy canyon floor. See figure 5 for legend and figure 1 for core location.

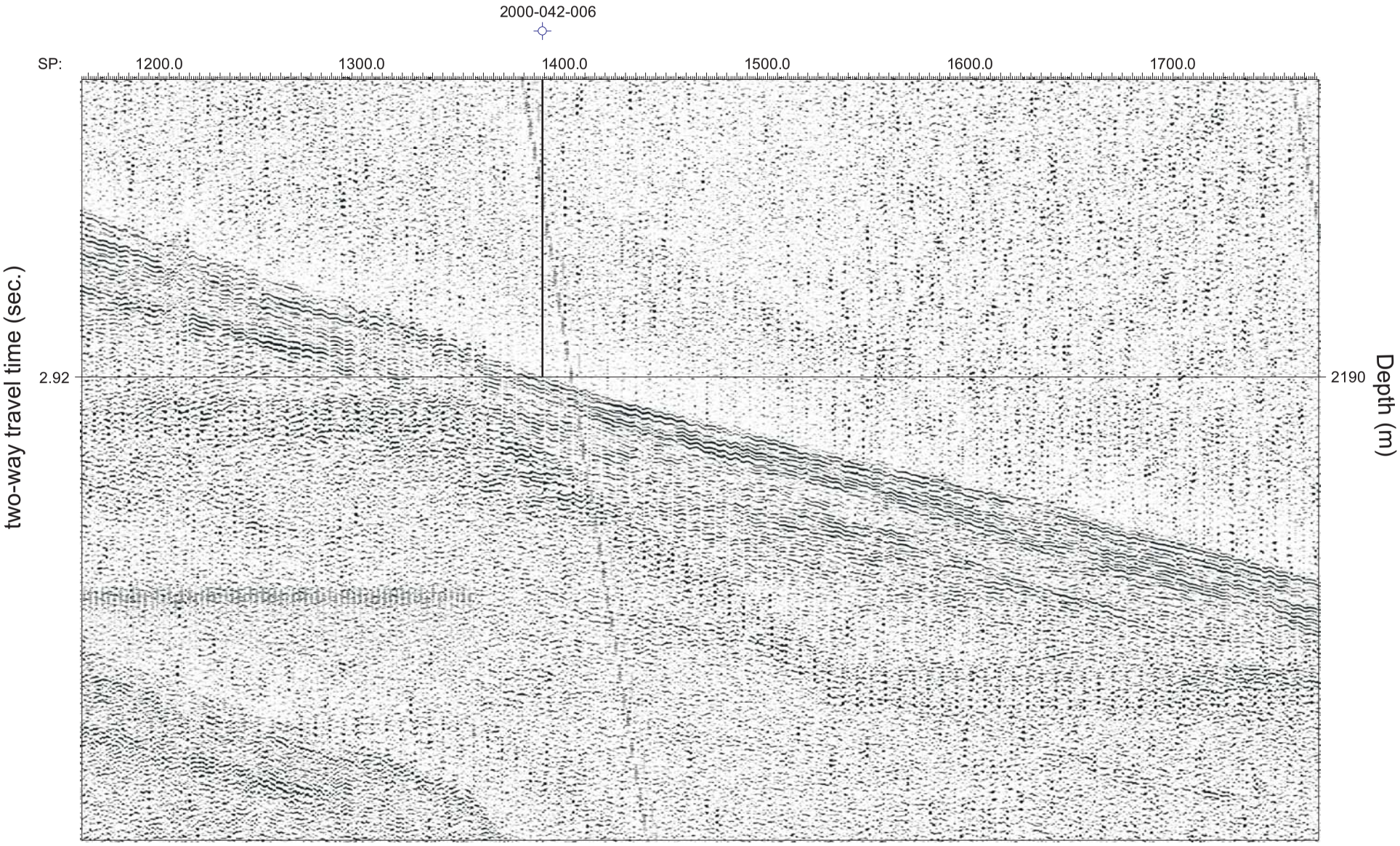

Figure 14: Huntec seismic reflection profile from a canyon floor showing core site 2000-042 006. See figure 1 for location of core site.

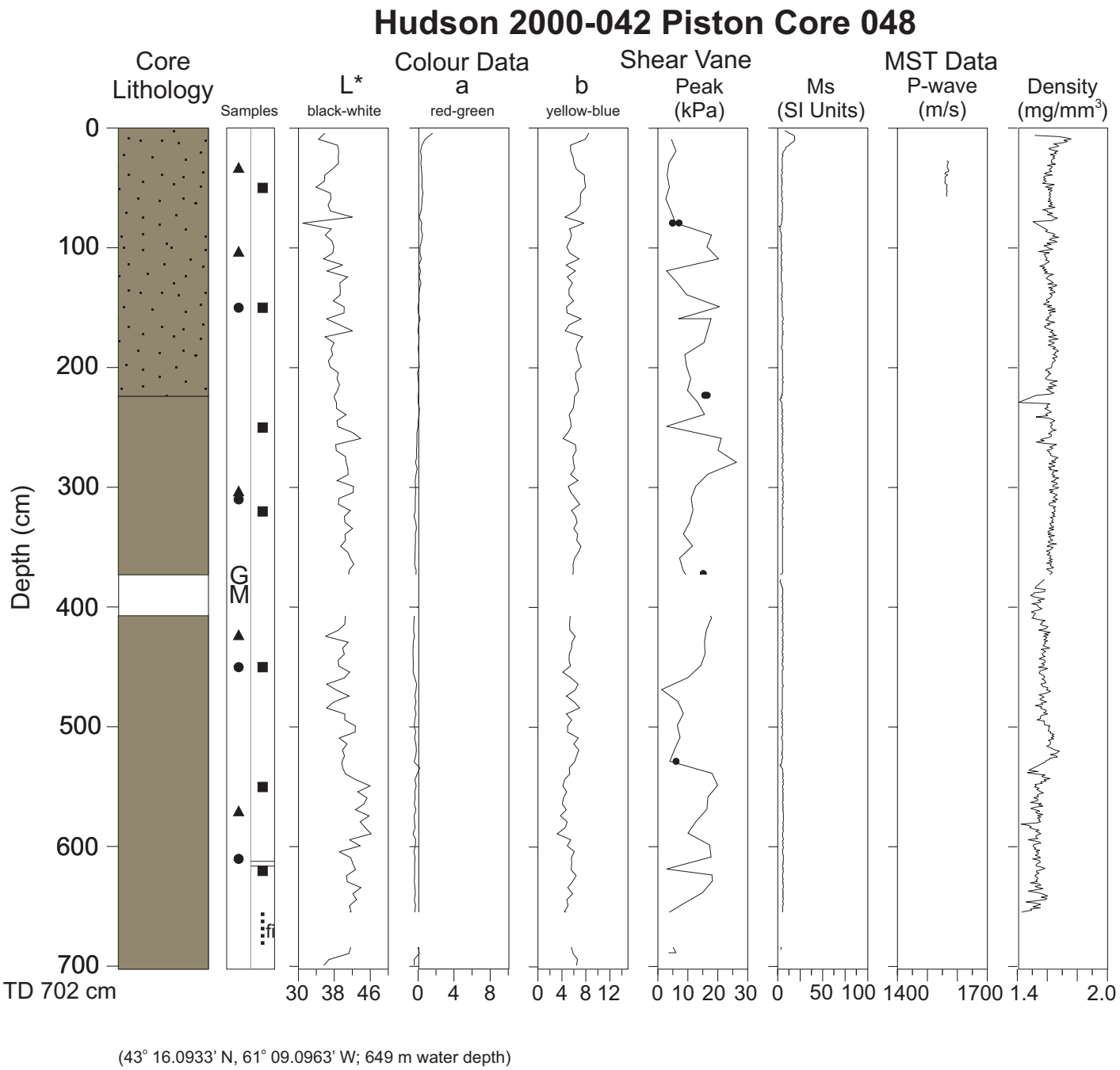

Figure 15: Downcore lithological and physical properties plot for core 2000-042 048 taken from a sandy canyon floor. See figure 5 for legend and figure 1 for core location.

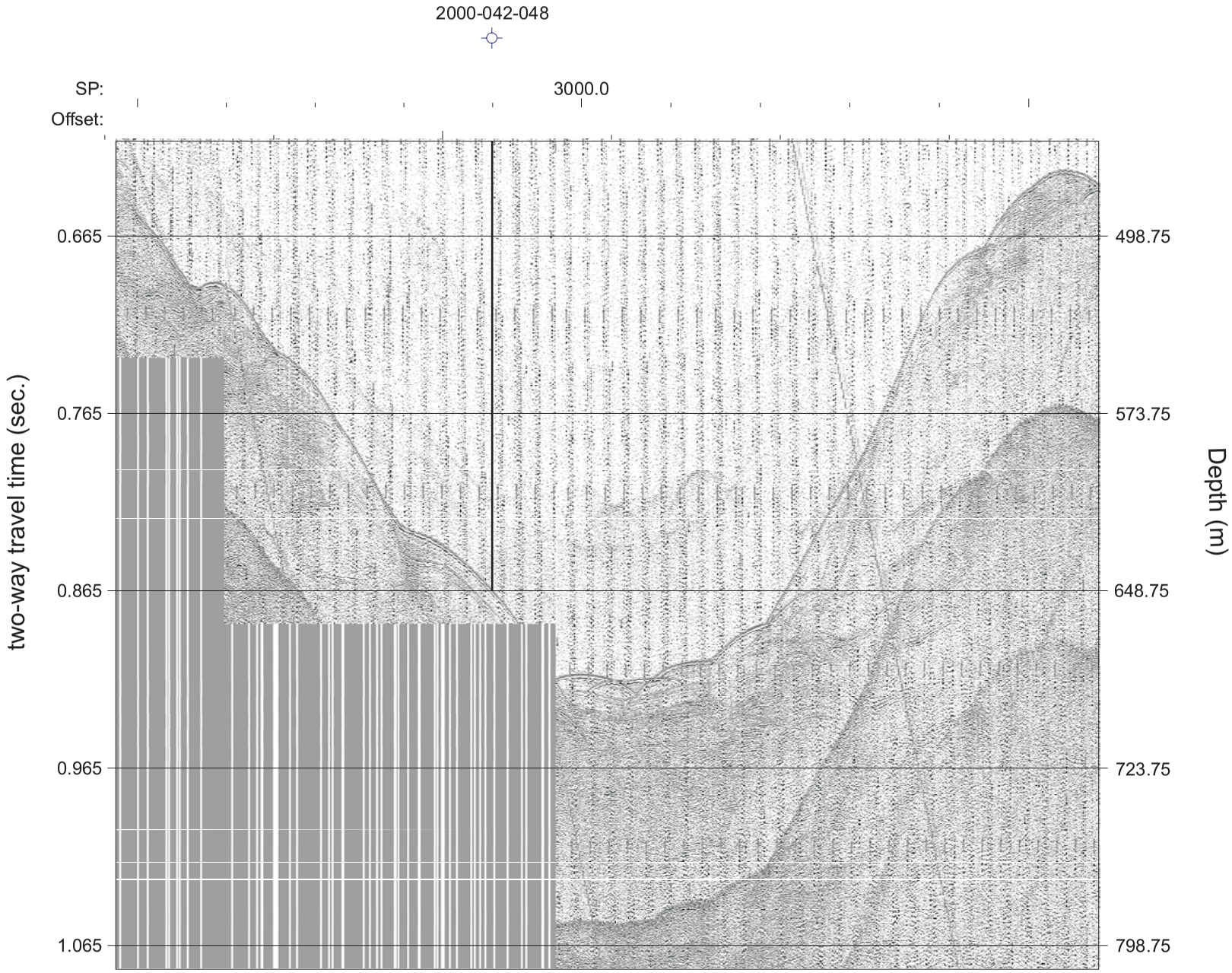

Figure 16: Huntec seismic reflection profile from a sandy canyon floor showing core site 2000-042 048. See figure 1 for location of core site.

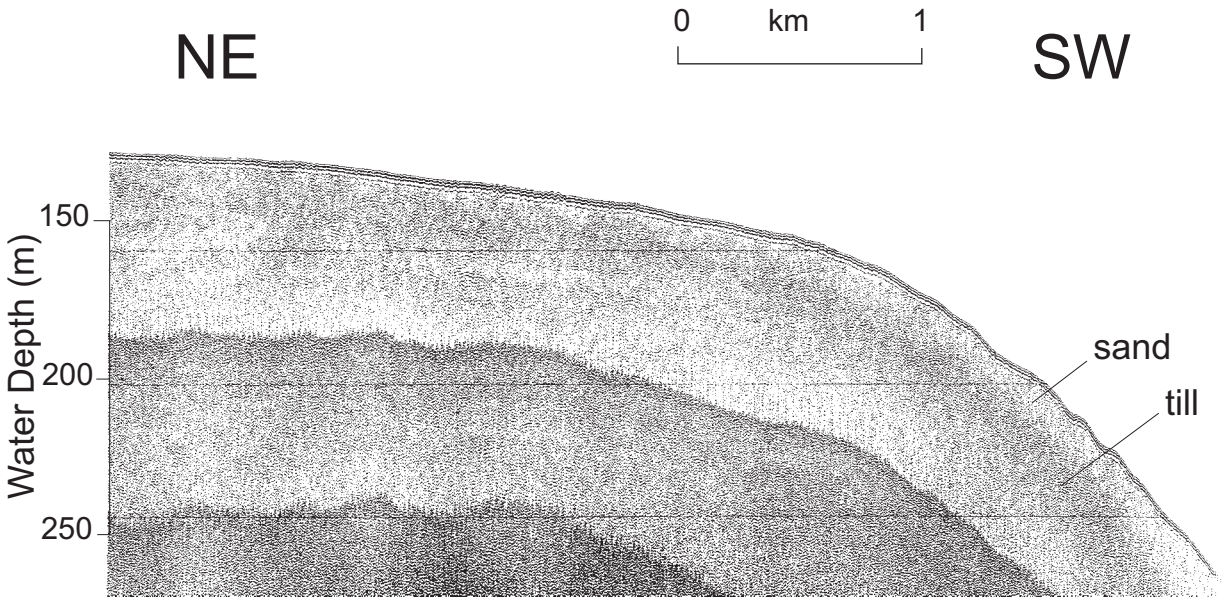

Figure 17: Huntec seismic reflection profile near the head of Dawson Canyon showing sand over probable till (modified from Piper and Campbell (2002)).

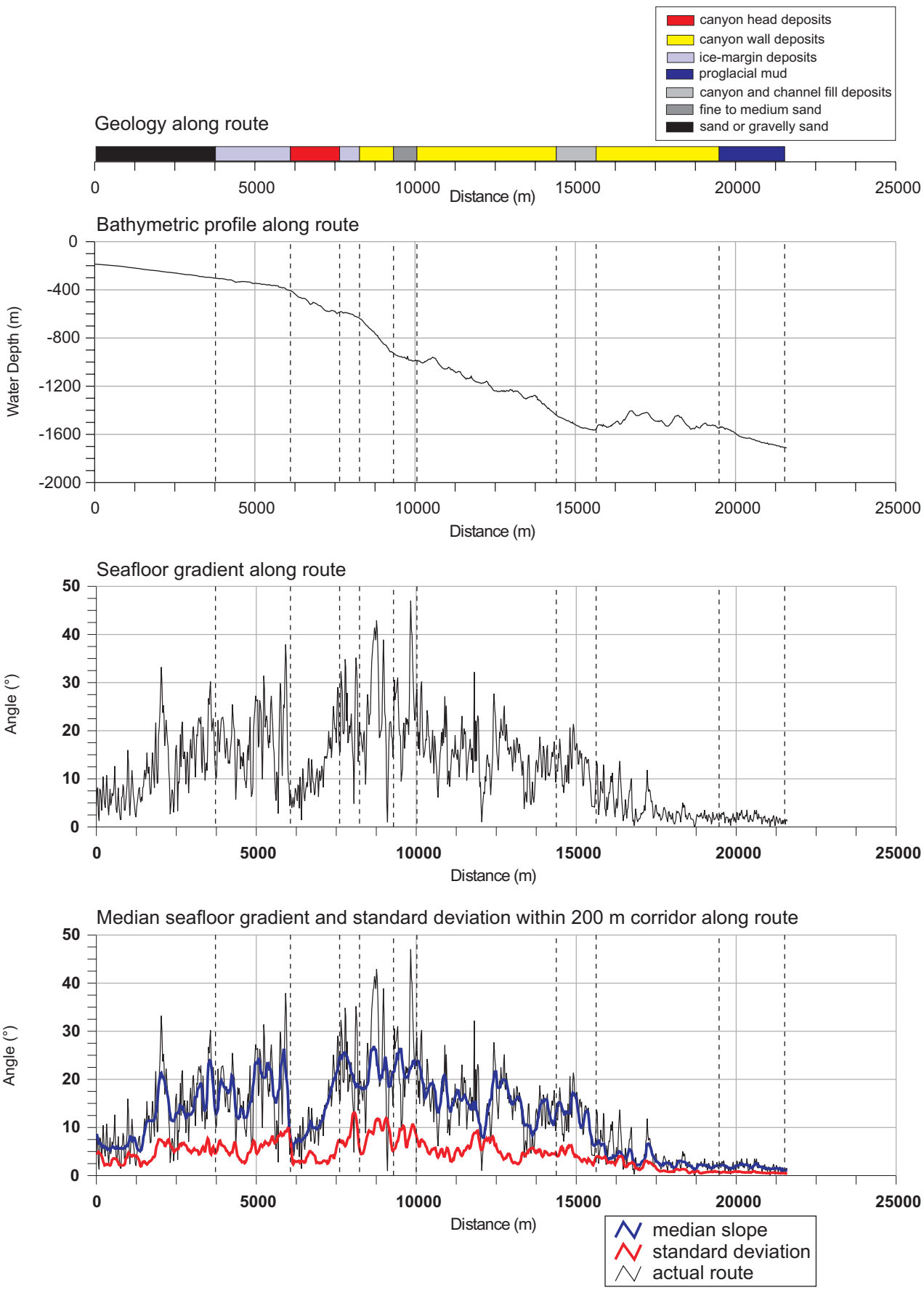

Figure 18: Surficial geology,water depth, seafloor gradient, and gradient statistics within a 200m corridor, Route 1.

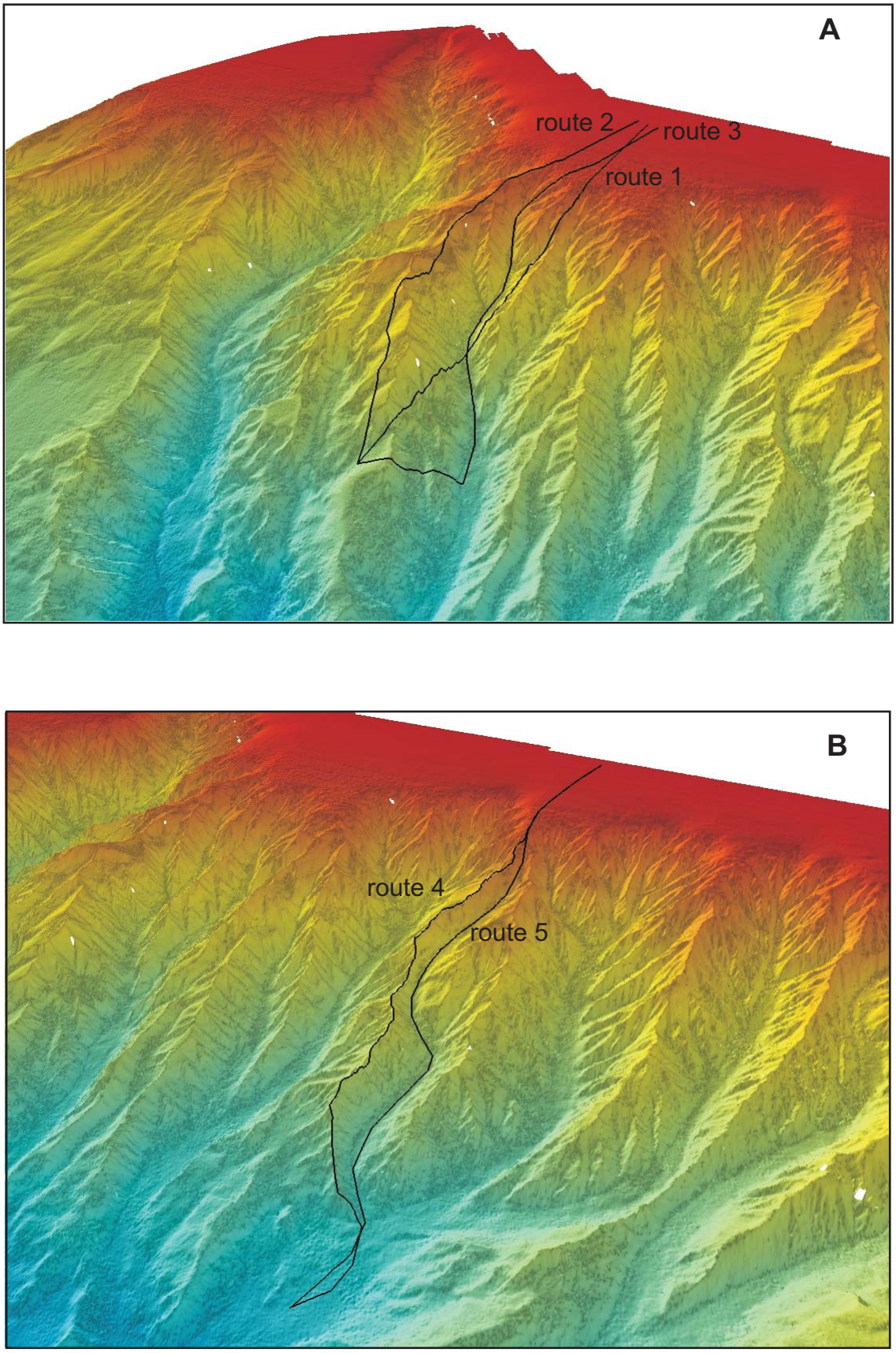

Figure 19: Perspective view of the seabed for A) routes 1-3, and B) route 4-5.

Deepwater Pipeline Route: Intercanyon Ridge- Annapolis Field to the Outer Shelf

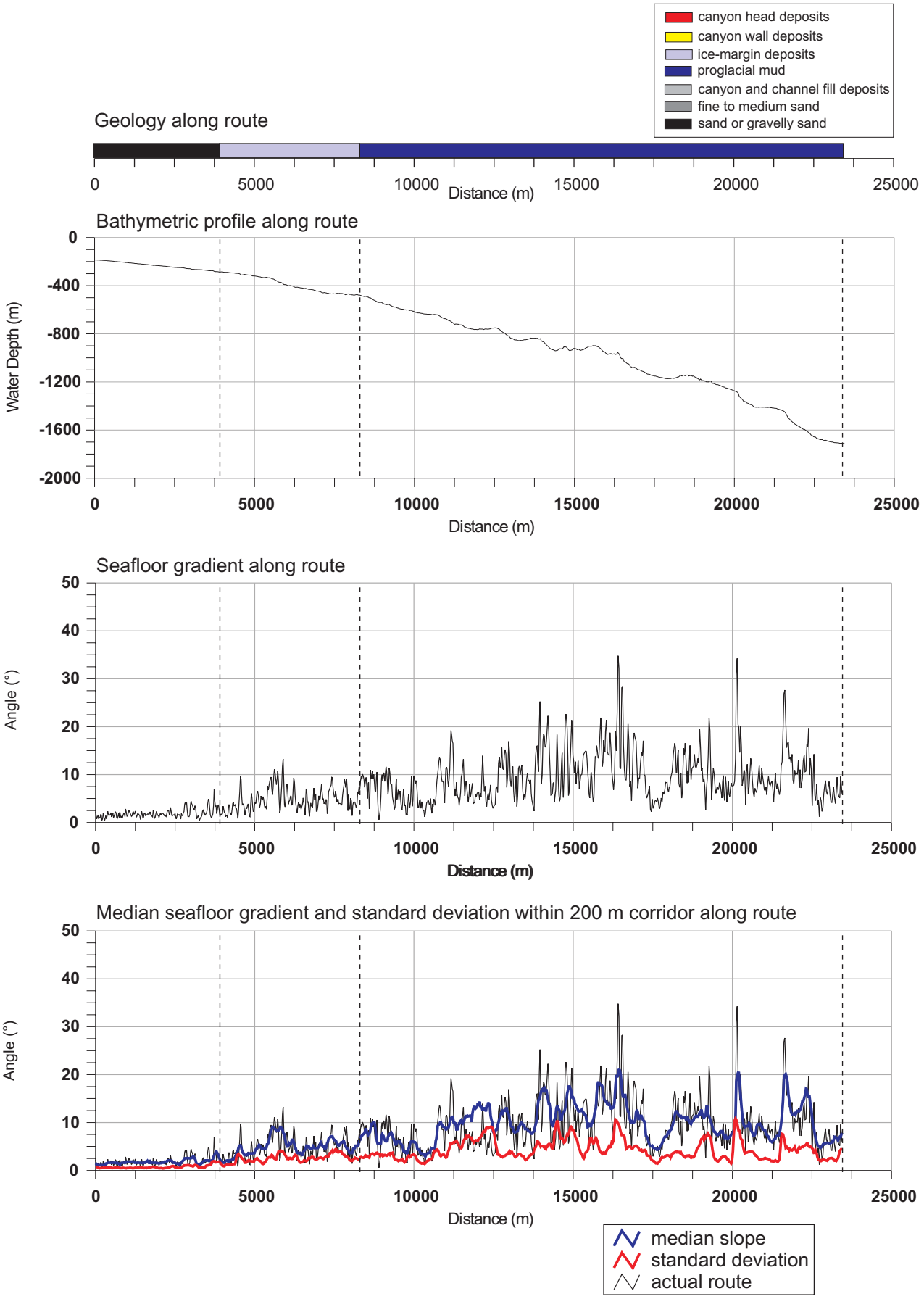

Figure 20: Surficial geology,water depth, seafloor gradient, and gradient statistics within a 200m corridor, Route 2.

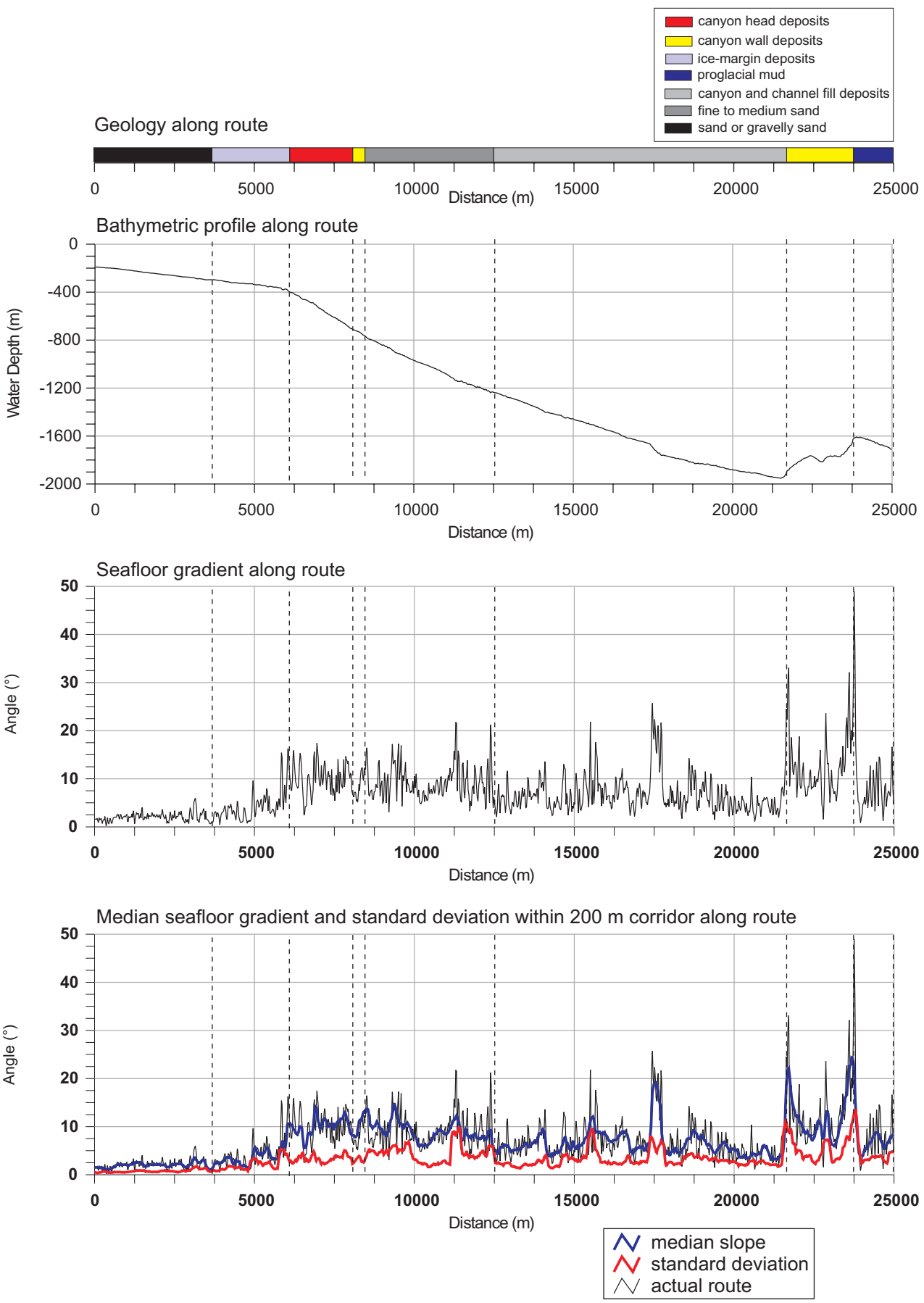

Figure 21: Surficial geology,water depth, seafloor gradient, and gradient statistics within a 200m corridor, Route 3.

Deepwater Pipeline Route: Intercanyon Ridge- Arbitrary Location to the Outer Shelf

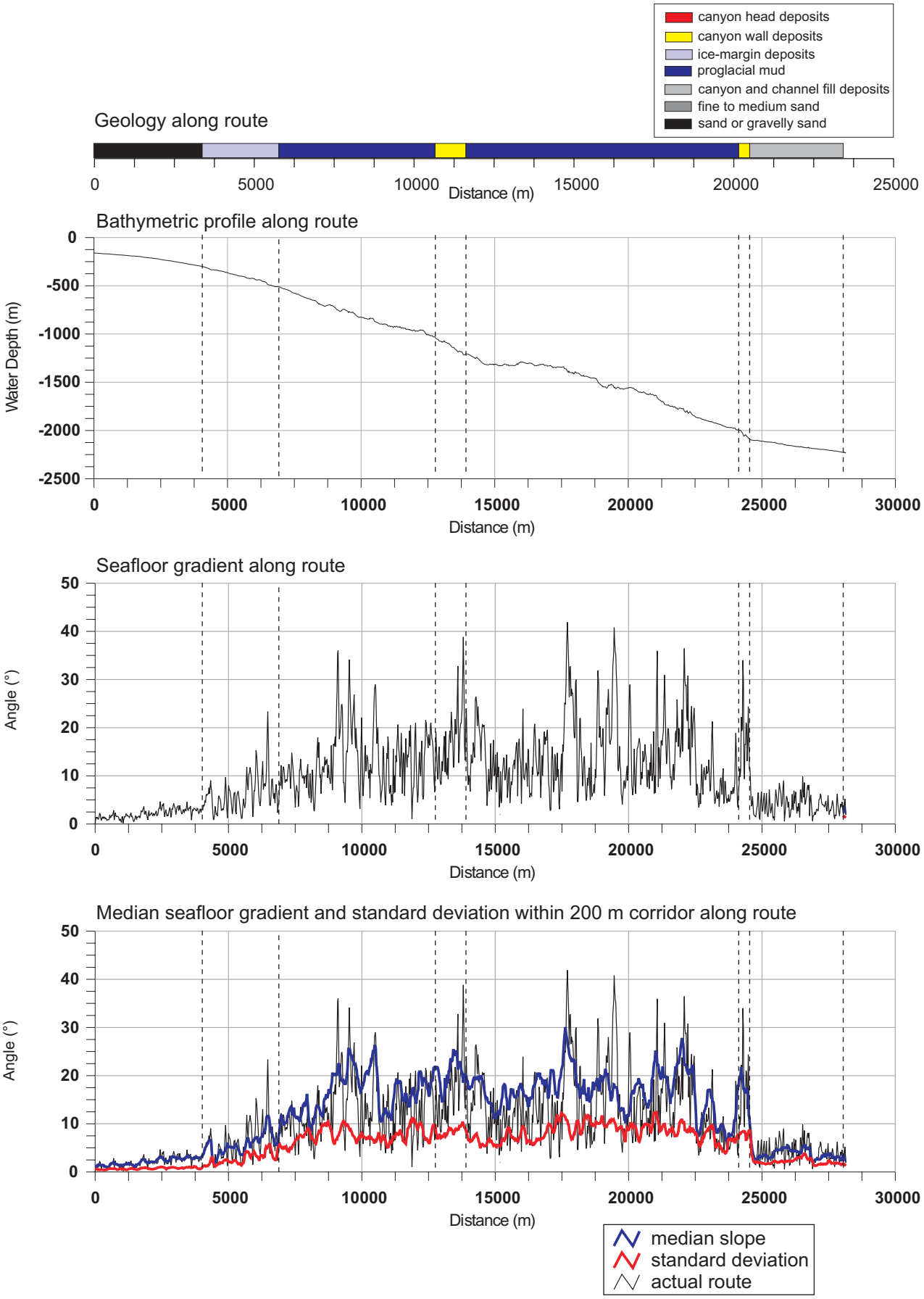

Figure 22: Surficial geology,water depth, seafloor gradient, and gradient statistics within a 200m corridor, Route 4.

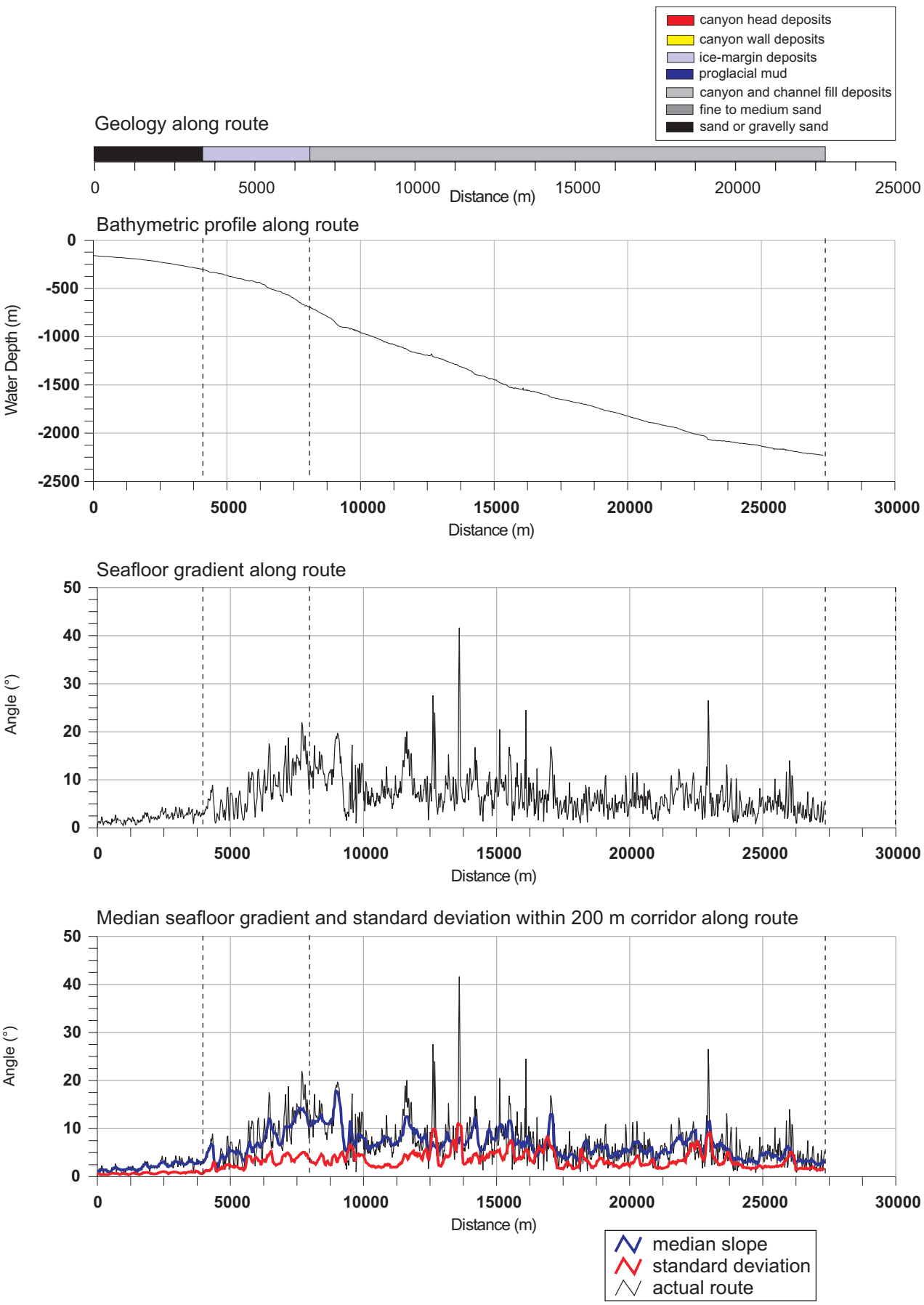

Figure 23: Surficial geology,water depth, seafloor gradient, and gradient statistics within a 200m corridor, Route 5.

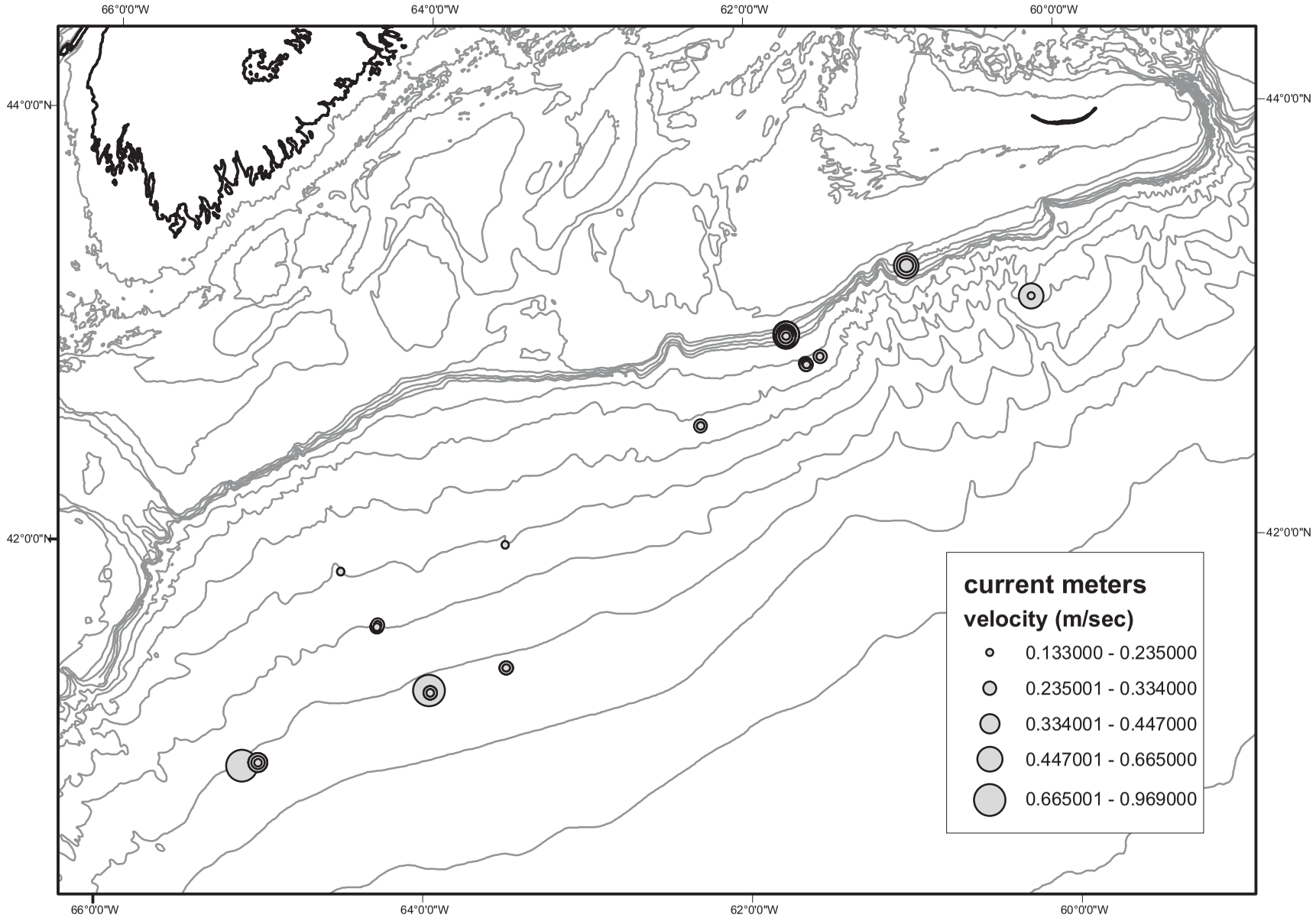

Figure 24: Current meter locations and current velocities for measurements within 150 m of the seafloor for the Scotian Slope.

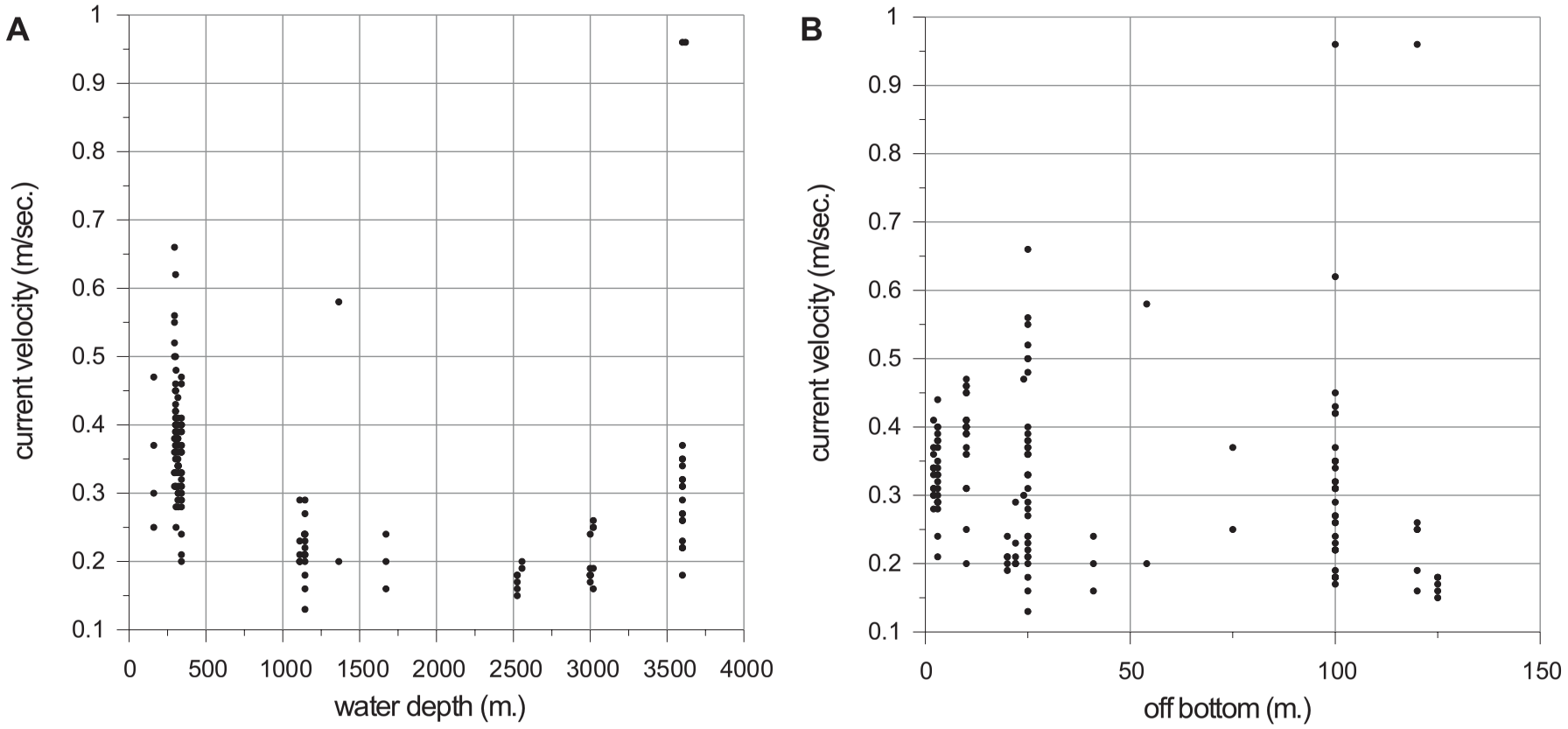

Figure 25: Current velocities A) current velocity versus water depth for measurements within 150 m of seabed, B) current velocity versus distance off the seafloor for measurements in A.

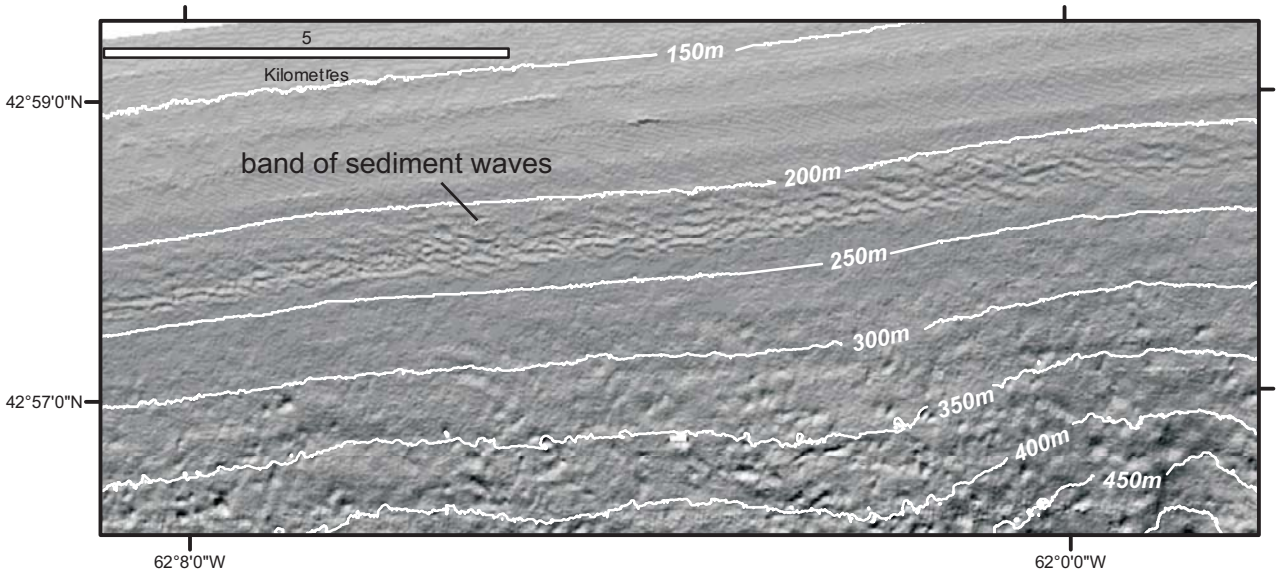

Figure 26: Bedforms on the upper slope, west of the study area.

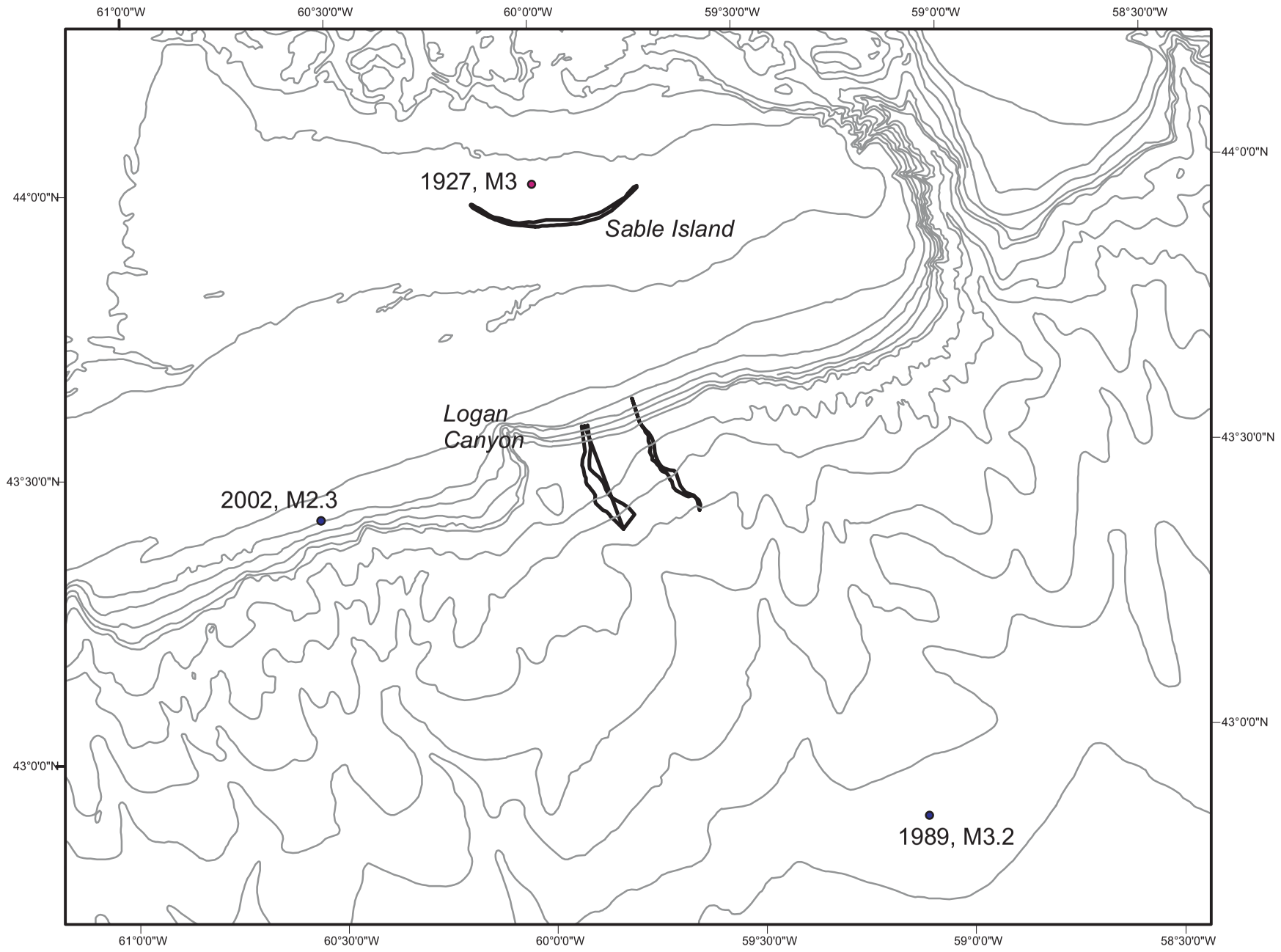

Figure 27: Location of seismic events within 100 km of study area (year, magnitude) from the National Earthquake Database.